UNIVERSIDADE FEDERAL DE MINAS GERAIS

FACULDADE DE FARMÁCIA

PROGRAMA DE PÓS-GRADUAÇÃO EM CIÊNCIAS FARMACÊUTICAS

MARCELA COELHO SILVA RIBEIRO

Lipoplex functionalization with hyaluronic acid for safe and efficient delivery of siRNA to the retina

Belo Horizonte – MG

2019

MARCELA COELHO SILVA RIBEIRO

Lipoplex functionalization with hyaluronic acid for safe and efficient delivery of siRNA to the retina

Thesis, as a partial requirement for the degree of Doctor in Pharmaceutical Sciences, submitted to the Postgraduate Program in Pharmaceutical Sciences from the Faculty of Pharmacy of the Federal University of Minas Gerais.

.

Advisor: Prof. Dr. Armando da Silva Cunha Júnior
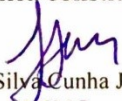
Belo Horizonte – MG

2019

FOLHA DE APROVAÇÃO

Lipoplex functionalization with hyaluronic acid for safe and efficient delivery of siRNA to the retina

MARCELA COELHO SILVA RIBEIRO

Tese submetida à Banca Examinadora designada pelo Colegiado do Programa de Pós-Graduação em CIÊNCIAS FARMACÊUTICAS, como requisito para obtenção do grau de Doutora em CIÊNCIAS FARMACÊUTICAS, área de concentração CIÊNCIAS FARMACÊUTICAS.

Aprovada em 29 de maio de 2019, pela banca constituída pelos membros:

Prof. Armando da Silva Cunha Junior - Orientador
UFMG

Profa. Gisele Rodrigues da Silva
UFOP

Prof. Frederico Pittella Silva
UFJF

Profa. Caryne Margotto Bertollo
UFMG

Profa. Anna Eliza Maciel de Faria Mota Oliveira
UNIFAP

Belo Horizonte, 29 de maio de 2019.

Dedico este trabalho:

À minha família, em especial aos meus pais e meu irmão, pelo incentivo constante e apoio incondicional.

AGRADECIMENTOS

Agradeço a Deus, por me guiar e possibilitar esta realização profissional na minha vida.

Ao meu orientador Prof. Dr. Armando da Silva Cunha Júnior, pelos ensinamentos, dedicação, amizade, por acreditar no meu trabalho e proporcionar oportunidades para o meu crescimento acadêmico.

Aos meus queridos pais, Leonardo e Janúlia, por não medirem esforços para que esse trabalho fosse possível. Eu tenho por vocês um enorme respeito, carinho e admiração. Ao meu irmão Daniel, por ser meu melhor amigo e estar sempre presente em todos os momentos importantes da minha vida. A Matheus Viana Braz, por seu amor e companheirismo, essenciais para a conclusão desse trabalho.

A equipe Biothérapies par Vectorization d'Acides Nucléiques – Université Paris Descartes, pelo acolhimento e colaborações prestadas a este trabalho. À Christine Charriou pelos conselhos, amizade e conhecimentos compartilhados. Em especial à Virginie Escriou pela confiança, orientação e toda infraestrutura cedida, que de maneira singular, contribuiu decisivamente para a realização deste trabalho.

A equipe do Laboratório de Imunologia Celular e Molecular do Instituto de Ciências Biológicas e ao Prof. Dr. Dawidson Assis Gomes pela colaboração nos testes celulares *in vitro*. Em especial, eu gostaria de agradecer ao doutorando Marcelo Miranda por suas importantes contribuições, pela amizade e prestatividade diante de tantos desafios que surgiram.

Aos meus colegas de laboratório: Pedro, Graci, Cleildo, Keren, Grazi, Mayara, Rummenigue, Carol, Nayara, Raquel, Cibele, Lays, Lorena, Flávia, Brenda, Eliza e Ana Luiza, pelo apoio, aconselhamentos e momentos de descontração.

A Iara e Luiza, pela agradável convivência e amizade.

" O desejo vence o medo, atropela

inconvenientes e aplana dificuldades".

(Mateo Alemán)

RESUMO

Desde que o silenciamento de genes específicos relacionados a doenças na retina tornou-se uma realidade com o uso de pequenos RNAs interferentes (do inglês, small interfering RNAs – siRNAs), essa tecnologia tem sido amplamente estudada para promover o tratamento ou até mesmo a cura de distúrbios oculares de origem genética. Apesar dos recentes avanços, o sucesso clínico do silenciamento gênico na retina é significativamente limitado por barreiras anatômicas e fisiológicas do olho. Além disso, as moléculas de siRNA não conseguem atravessar livremente as membranas celulares em função de seu peso molecular e carga negativa. Com base no exposto, o objetivo deste trabalho foi desenvolver um nanocarreador à base de lipídios (lipoplex), estrategicamente revestido com ácido hialurônico (AH) para facilitar a internalização de siRNAs nas células da retina. Diferentes pesos moleculares de AH (8-15 kDa e 160-600 kDa) foram avaliados para a funcionalizar a superfície do lipoplex catiônico e as partículas obtidas foram caracterizadas por espalhamento dinâmico de luz e microscopia eletrônica de transmissão. O lipoplex catiônico evidenciou um diâmetro médio de 133,5 ± 1,2 nm e um potencial zeta de 71,1 ± 3,0 mV. Após a adição de AH (160-600 kDa), tanto o tamanho quanto o potencial zeta foram estatisticamente diferentes em comparação aos lipoplexes não modificados (p> 0,05), evidenciando um diâmetro médio de 221,8 ± 9,2 nm e um potencial zeta de - 34,2 ± 1,4 mV. Esses resultados associados à caracterização morfológica das nanopartículas indicaram uma ligação eletrostática entre o lipoplex e AH. Além disso, estudos *in vitro* e eletroforese foram realizados para verificar se o revestimento de AH poderia interferir na incorporação de siRNA no lipoplex e em sua eficácia. Os lipoplexes revestidos com AH não só protegeram o siRNA como também facilitaram sua internalização em células do epitélio pigmentado da retina, ARPE-19. Os resultados indicaram que o lipoplex modificado com AH foi capaz de introduzir as moléculas de siRNA (37,6 nM) nas células da retina sem apresentar uma citotoxicidade aparente. Diante disso, tanto a distribuiçao quanto a segurança do lipoplex catiônico e associado ao AH na retina foram investigadas em estudos *in vivo*. Ao contrário do lipoplex catiônico que não foi capaz de penetrar em camadas mais profundas da retina, o uso do lipoplex modificado com AH

apresentou sinais do siRNA fluorescente em diferentes camadas da retina. Além disso, ambos os sistemas não demonstraram efeitos tóxicos à retina após 7 e 14 dias das injeções intravítreas, de acordo com a eletrorretinografia, avaliação clínica e histologia dos olhos de ratos da linhagem Wistar. Considerando todos os resultados, o lipoplex revestido por ácido hialurônico pode ser um sistema promissor para promover a proteção e o transporte do siRNA para a retina.

Palavras-chaves: Lipoplex. Small interfering RNA (siRNA). Ácido hialurônico. Injeção intravítrea.

ABSTRACT

Since the possibility of silencing specific genes linked to retinal diseases has become a reality with the use of small interfering RNAs (siRNAs), this technology has been widely studied in order to promote the treatment or even the cure of genetic eye disorders. Despite the recent advances, the clinical success of gene silencing in the retina is significantly limited by inherent anatomical and physiological ocular barriers. Moreover, the siRNA molecules cannot freely cross cell membranes due to their relatively high molecular weight and negative charge. Therefore, this work aimed to develop a lipid-based nanocarrier (lipoplex) strategically coated with hyaluronic acid (HA) to penetrate vitreous space and facilitate siRNAs internalization into retinal cells. Different molecular weights of HA (8-15 kDa and 160-600 kDa) were evaluated for cationic lipoplex surface functionalization and the obtained particles were characterized by dynamic light scattering and transmission electron microscopy. Cationic lipoplex had a Z-average diameter of 133.5 ± 1.2 nm and zeta potential of 71.1 ± 3.0 mV. Upon addition of HA (160-600 kDa), both size and zeta potential were statistically different compared to non-modified lipoplexes ($p > 0.05$), showing a Z-average diameter of 221.8 ± 9.2 nm and zeta potential of - 34.2 ± 1.4 mV. These results and morphological characterization indicated an electrostatic binding between lipoplex and HA. In addition, electrophoresis and *in vitro* studies were performed to evaluate if HA coating could interfere in siRNA incorporation into lipoplex and their efficacy. HA-coated lipoplexes could protect siRNA and also facilitate its internalization into a human retinal pigment epithelial cell line, ARPE-19. Our findings indicate that HA-lipoplexes were able to introduce siRNA molecules (37,6 nM) in retinal cells without apparent cytotoxicity. Based on this, *in vivo* retinal distribution and safety of cationic and HA-lipoplex were also investigated. In contrast to the cationic lipoplex that was not able to penetrate deeper retinal structures, HA-coated lipoplexes showed a clear localization of fluorescent siRNA signal in the inner and outer nuclear layer of retina. Moreover, both systems showed no toxic effects to the retina after 7 and 14 days of intravitreal injections, according to electroretinography, clinical evaluation, and histology of Wistar rat's eyes. Considering all the results, the

lipoplex coated with hyaluronic acid may represent a promising approach to promote the protection and transport of the siRNA to the retina.

LIST OF FIGURES

Chapter 01

Chapter 02

Figure 02- Acrylamide gel electrophoresis analysis of naked siRNA and lipoplexes, covered or not with hyaluronic acid. Each sample contains 0.3 µg of siRNA, electrophoresed through 8% acrylamide gel at 90 V for 40 min. (1) Band of intact naked double-stranded siRNA; (2) naked double-stranded siRNA after the treatment with Triton X-100 and NaCl 1 M solution; (3) siRNA complexed in the cationic lipoplex without treatment; (4) Band of siRNA released from uncoated lipoplex, after the treatment for

and HA-lipoplex. The siRNA without fluorescence was used as a control. Transfection results were normalized with cells protein concentration (n=3). Error bars represent the standard deviation (*) p <0.005 compared to the untreated cells (One-way ANOVA and post-test of Bonferroni). (B) Fluorescence intensity of ARPE-19 cells after incubation with RFP plasmids associated with HA-lipoplex and Lipofectamine®.

Chapter 03

LIST OF ABBREVIATIONS

AA	Alginic Acid
BCA	Bicinchoninic acid
bp	base pairs
BSA	Bovine Serum Albumin
Cryo-TEM	Cryogenictransmission electron microscopy
Da	Dalton
DLS	Dynamic Light Scattering
BSA	Bovine Serum Albumin
BRB	Blood-retinal barrier
DMAPAP	2-{3-[Bis-(3-amino-propyl)-amino]-propylamino}-N ditetradecylcarbamoyl methyl-acetamide
DMEM-F12	Dulbecco modified Eagle's minimal essential medium
DNA	Desoxyribonucleic acid
DOPE	1,2-diesteroil-sn-glycero-3-phosphoethanolamine
DOTAP	N-[1-(2,3-Dioleoyloxy)propyl]-N,N,N-trimethylammonium
dsDNA	double-strand DNA
ERG	Electroretinography
FDA	Food and Drug Administration
HA	Hyaluronic acid
ISCEV	International Society for Clinical Electrophysiology of Vision
IOP	Intraocular pressure
kDa	kilodalton
LED	Light Emitting Diodes
LUV	Large Unilamellar Vesicles
mRNA	Messenger RNA
miRNA	Micro RNA
MLV	Multilamellar Vesicles

Ms	Milliseconds
MTT	3-(4,5-dimethylthiazol-2-yl)-2,5-diphenyltetrazolium bromide
mV	milliVolts
MV	Multivesicular Vesicles
Mw	Molecular weight
NaCl	Sodium chloride
nm	Nanometer
NP	Nanoparticle
pDNA	Plasmid DNA
pAd-RFP	Plasmid RFP
PDI	Polydispersity index
PE	Polyethylene
PEI	Polyethyleneimine
PEG	Polyethylene glycol
REV	Reverse-phase evaporation
Rhod	Rhodamine
RPE	Retinal Pigmented Epithelium
RPE65-LCA	RPE65-Leber congenital amaurosis
RNA	Ribonucleic acid
RNAi	RNA interference
RISC	RNA-inducible silencing complex
R +/-	Positive/negative charge ratio
SAXS	Small Angle X-ray Spectroscopy
siRNA	Small interfering RNA
shRNA	Short hairpin RNA
SUV	Small Unilamellar Vesicle
TBE	Tris/Borate/EDTA buffer
TBE	Tris/Borate/EDTA buffer
TEM	Transmission Electron Microscopy

μA	Microampere
μV	Microvolt
VIP	Vasoactive Intestinal Peptide
v/v	volume/volume
w/w	weight/weight

SUMMARY

GENERAL INTRODUCTION

Since its discovery, RNA interference has been widely studied to identify new molecular targets and elucidate gene function. Recent advances in the preclinical and clinical use of small interfering RNAs (siRNAs) have shown their potential therapeutic applications as an inhibitor of gene expression in many diseases, including retinal degenerations. The intraocular administration of siRNAs is related to several obstacles as the difficulty in penetrating target cells and their fast degradation in biological media. Therefore, viral and non-viral vectors have been applied to improve therapeutic efficacy and address these limitations. This work focuses on the development of a non-viral vector called lipoplex. These lipoplexes were functionalized by hyaluronic acid (HA) aiming to protect siRNA against degradation and improve its internalization into the retinal tissues. The present thesis consists of three parts, according to the following plan:

Chapter one is a bibliographic review focus on RNAi therapy strategies targeting the eye, including ocular physiological barriers, siRNA delivery systems limitations and recent improvements.

Chapter two is the first experimental part of this work, which contains the development and characterizing of lipoplex and *in vitro* related studies in retinal cells.

Chapter three shows the *in vivo* distribution and safety of lipoplex in rat retina.

PURPOSE

GENERAL PURPOSE

The present study aims to develop siRNA lipoplexes strategically coated with hyaluronic acid (HA) to facilitate their mobility into the vitreous humor and obtain a safe and efficient *in vivo* delivery of siRNA to retinal tissues.

SPECIFIC PURPOSE

Chapter 2

- ✓ Development of cationic lipoplexes functionalized with hyaluronic acid by using electrostatic binding.
- ✓ Physicochemical characterization of lipoplex by dynamic light scattering (DLS), transmission electron microscopy (TEM) and cryogenic transmission electron microscopy (cryo-TEM).
- ✓ Detection of CD44 expression on ARPE-19 cells.
- ✓ *In vitro* uptake of lipoplex by human retinal pigment epithelial cell line (ARPE-19).
- ✓ Cytotoxic evaluation of lipoplex in retinal cells.
- ✓ *In vitro* transfection efficiency of lipoplex.

Chapter 3

- ✓ *In vivo* toxicity investigation of lipoplex administrated by intravitreal injections in rat retina through electroretinogram (ERG), clinical evaluation and histological analyses.
- ✓ Retinal distribution of lipoplex after intravitreal injections by confocal microscopy.

1.1 The anatomy and physiology of the eye

The human eye is an important sensory organ able to receive energy from light in the environment, convert it to electrical signals and transmit them through the optic nerve to the brain. The eye can be divided into two anatomical regions: the anterior and posterior segments. The anterior segment is composed of the cornea, conjunctiva, iris, lens, ciliary body and aqueous humor. The posterior segment contains the vitreous chamber, retina, choroid, posterior sclera and optic nerve (DELPLACE, PAYNE and SHOICHET, 2015; MOHLIN et al., 2017; DIAS et al., 2018). The main ocular structures are schematically demonstrated in **Figure 01**.
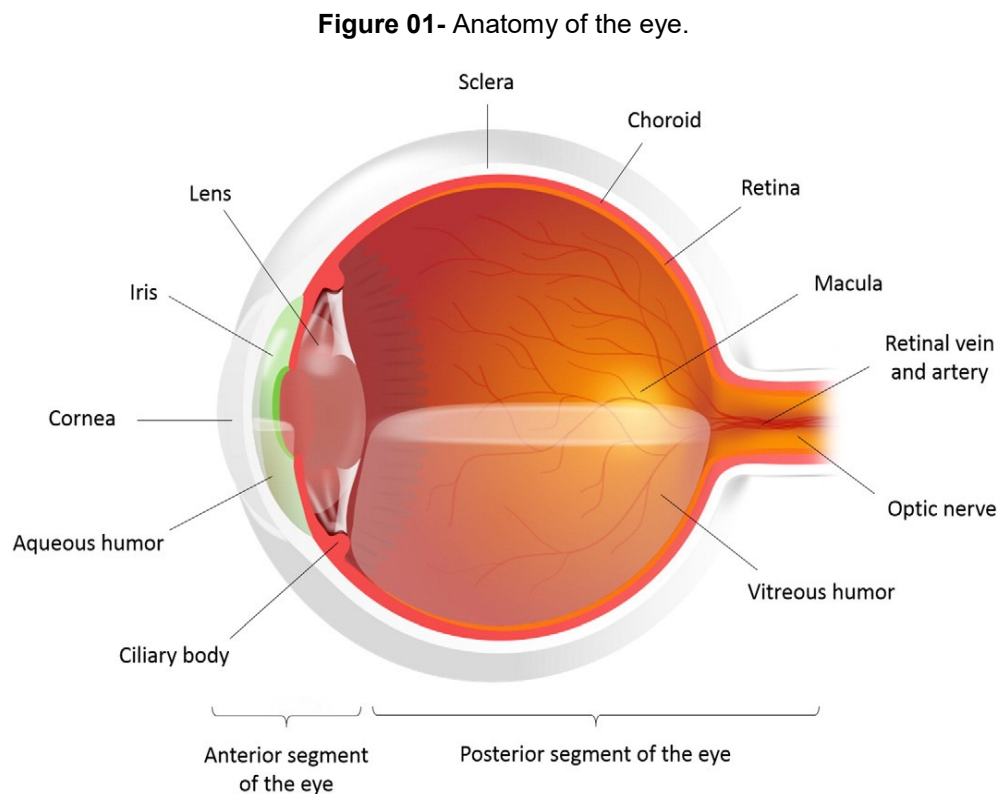
Figure 01- Anatomy of the eye.

DELPLACE, V.; PAYNE, S.; SHOICHET, M. Delivery strategies for treatment of age-related ocular diseases: From a biological understanding to biomaterial solutions. **Journal of Controlled Release**, v. 219, p.652-668, 2015.

1.2 Anterior segment of the eye

The cornea is a transparent avascular tissue that acts as a structural barrier, protecting the eye against infections. It is composed of five recognized layers: epithelium, stroma, endothelium, Bowman's membrane and Descemet's membrane. Although the cornea is a diffusional barrier, it is an essential route of anterior drug absorption. The ocular drug absorption from the lacrimal fluid to the anterior ocular tissues is mainly influenced by the drug permeability in this structure and the time in contact with the ocular surface. Moreover, the cornea and the tear film are essential refractive components of the anterior segment of the eye (MANNERMAA et al., 2006; DELMONTE and KIM, 2011; MA et al., 2018).

The sclera is the outermost layer of the eye, extending from the limbus at the margin of the cornea anteriorly to the optic nerve in the posterior segment of the eye. It is predominantly made up of collagen and serves as the attachment site for the extraocular muscles. Also, the sclera protects the intraocular structures and provides the final shape and size of the eye, showing limited distension and contraction to accommodate minor variations in intraocular pressure MALHOTRA et al., 2011; METLAPALLY and WILDSOET, 2015). The lens participates in the refractive mechanisms and allows the eye focusing of images. This structure is normally transparent, surrounded by an elastic capsule that deforms to perform the visual accommodation. The lens is avascular but receives nutrients from aqueous humor (PRESLAND and MYSATT, 2010).

The iris is a thin, contractile and pigmented structure, positioned between the cornea and the lens, with the pupil in the center. The pupil limits the entrance of the light into the eye and almost instantaneously contracts or expands according to the light exposition. The human iris color variation is due to differences in the amount and distribution of melanin. In the peripheral part of the iris, the ciliary body is responsible for the secretion of the aqueous humor from the posterior to the anterior segment. This fluid nourishes and oxygenates the adjacent avascular tissues. The production and drainage of aqueous humor should be balanced to maintain adequate intraocular pressure. The

aqueous humor drains out of the eye via the trabecular meshwork and Schlemm canal (MOHLIN et al., 2017).

1.3 Posterior segment of the eye

The vitreous chamber is positioned between the lens and the retina and represents two-thirds of the volume of the eye. The vitreous acts as a shock absorber and gives the eye structural support by keeping the retina flat against the Bruch's membrane. This chamber is filled with a thick transparent bio gel called the vitreous humor. The vitreous humor is mainly composed of a random network of collagen-fibrils, hyaluronic acid (HA) and proteoglycans. The HA is an anionic hydrophilic polymer that is the principal constituent of the vitreous humor extracellular matrix (MALHOTRA et al., 2011; WOJCICKI et al., 2012). Compared to the plasma, the average protein concentration in healthy human vitreous is low since it is comprised of approximately 99% of water. The vitreous contains both structural proteins (collagen II, IX and V/XI, fibrillin and cartilage oligomeric matrix protein) and non-structural proteins (albumin, immunoglobulin, complement proteins, globulins, transferrin) (DEL AMO et al., 2017).

The choroid is a highly vascularized layer that provides blood and nutrients to retinal cells. Besides these functions, the choroid vessels are known to regulate eye temperature and maintain the ocular pressure. The choroid is located between the sclera and the retina and extends from the ciliary body to the optic nerve. It is thicker in the posterior region and becomes gradually thinner as it approaches the anterior region (GOODMAN e GILMAN, 2012; DELPLACE, PAYNE and SHOICHET, 2015).

An acute visual perception relies on proper refraction or bending of light passing through the anterior to the posterior part of the eye and the reach the retina, a well-organized photosensitive tissue. The overall organization of the neural retina is composed of different anatomical layers and cell types, as illustrated in **Figure 02**. Visual signals initiate through parallel vertical pathways that are established at the synapse between photoreceptors and bipolar cells. Then, these signals are transmitted to retinal ganglion

cells and propagate to the higher visual centers in the brain via the optic nerves (axons of the ganglion cells). In this process, glial (Müller and astrocytic) cells process visual information and provide metabolic support (DELPLACE, PAYNE and SHOICHET, 2015).

Figure 02 – Cellular architecture of the retina.
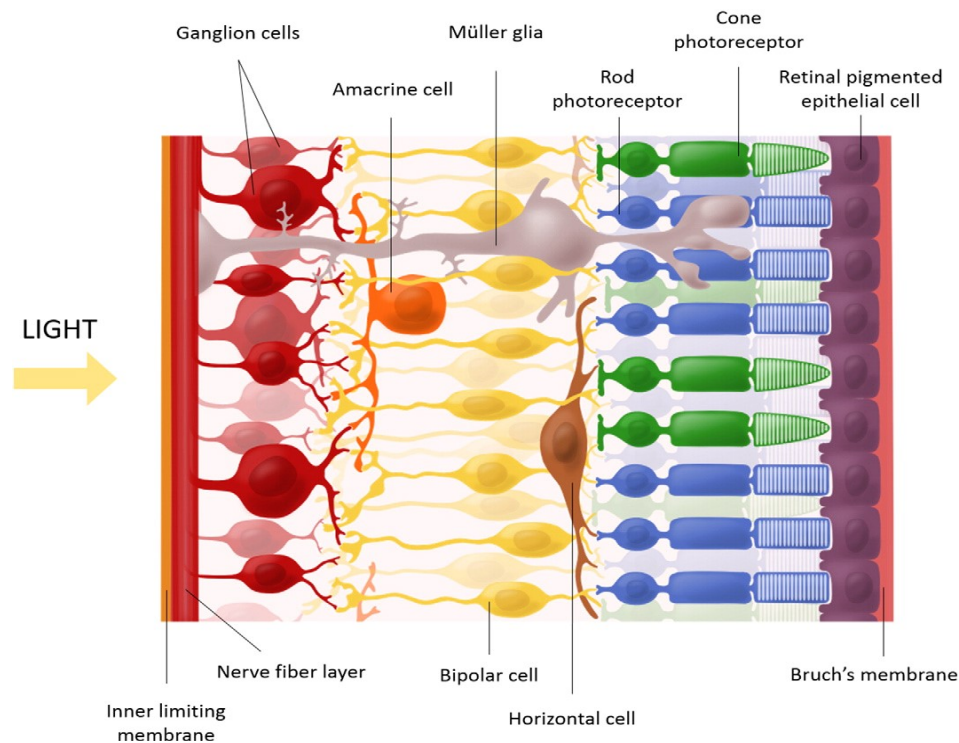
DELPLACE, V.; PAYNE, S.; SHOICHET, M. Delivery strategies for treatment of age-related ocular diseases: From a biological understanding to biomaterial solutions. **Journal of Controlled Release**, v. 219, p.652-668.

The photoreceptors can be broadly categorized into rods and cones. Rods have a refined sensitivity to light and can detect even a single photon, thus they are responsible for dim-light vision. By contrast, cones are 100 times less sensitive than rods and exhibit much faster response kinetics during phototransduction and can provide high acuity color vision. Therefore, different wavelengths of light can be specifically detected in each cone photoreceptor type. In the human macula, cone photoreceptors are densely packed while rods predominate in the peripheral region. The progressive loss of function

of photoreceptors is reported as a major cause of blindness in retinal degenerative diseases (YUE et al., 2016; OLIVEIRA, ROSA DA COSTA and SILVA, 2017).

The retinal pigment epithelium (RPE) is a monolayer located in the basement of the retina, which cells are joined to each other by tight junctions. This arrangement limits the intercellular trafficking of molecules and forms an important physiologic barrier of the eye, the blood-retinal barrier (BRB). Additionally, RPE is involved essential functions in the homeostasis of the retina such as recycling the visual pigments and maintaining the health of photoreceptors (DEL AMO et al., 2017; HUANG, CHEN and RUPENTHAL, 2018).

1.4 RNA interference

The RNA interference (RNAi) is a conserved biological mechanism essential to regulate gene expression and mediate resistance to endogenous parasitic or exogenous pathogenic nucleic acids. Fire et al. (1998) were the first to demonstrate that long double-stranded RNA (dsRNA) mediate RNAi in the nematode worm Caenorhabditis elegans, by driving a target messenger RNA (mRNA) to degradation. Later, the RNAi pathway was also shown to occur in different mammalian cell lines by inhibition of endogenous and heterologous gene expression, including human embryonic kidney and HeLa cells (ELBASHIR et al., 2001). Since its discovery, RNAi has advanced as a powerful tool to achieve highly specific gene inhibition. Among different post-transcriptional strategies, the most common molecules used to downregulate the gene of interest expression are the small interfering RNAs (siRNAs). siRNAs are double-stranded RNA oligonucleotides of 19-21 base pairs that offer the possibility of a potent, selective and long-lasting therapeutic effect for gene-related diseases. Moreover, these molecules are synthesized and do not require cellular expression systems or complex protein purification systems, making the time and costs of siRNA technology relatively low (WHITEHEAD et al., 2009; XIA et al., 2016; YU-WAI-MAN et al., 2016).

RNA mechanism leads to a sequence-specific post-transcriptional gene silencing. Within the intracellular compartment of eukaryotic cells, an endogenous ribonuclease RNase III enzyme (Dicer) metabolizes longer double-stranded RNA precursors to origin siRNA molecules. Then, siRNAs assemble into a multiprotein complex, termed RNA-induced silencing complex (RISC). When siRNA binds to RISC, the duplex siRNA is unwound by helicase, resulting in two single strands. The guide strand remains attached to RISC and binds to the targeted RNA molecule, while the passenger strand is removed. Following binding, a cleavage enzyme comprised in RISC called argonaut 2, degrades the target RNA and inhibits gene expression **(Figure 03)** (SARETT et al., 2015; SHEN et al., 2018).

Although this technique can specifically silence the expression of any chosen gene, different barriers to the intracellular delivery of siRNA significantly limit its clinical efficacy. One of the major limitations for the siRNA molecules is the inability to cross cell membranes and reach the cytoplasm. Besides their large molecular weight, the negative charges arising from the phosphate groups in the siRNA backbone electrostatically repel negatively charged cell membranes, interfering in their cell internalization. Also, the presence of endonucleases and exonucleases into the cell or body fluids can rapidly degrade siRNAs. To improve their pharmacologic properties, nuclease-resistant modifications (for example, phosphorothiolation or 2'-OMethyl RNA bases) can be introduced into oligonucleotides slated. Even so, new delivery systems are still needed to facilitate the internalization of siRNA into target cells for therapeutic use (HAMOUDI et al., 2015; YU-WAI-MAN et al., 2016; XIA et al., 2016; ARRUDA et al. 2019).

Figure 03 – siRNA structure and mechanism.
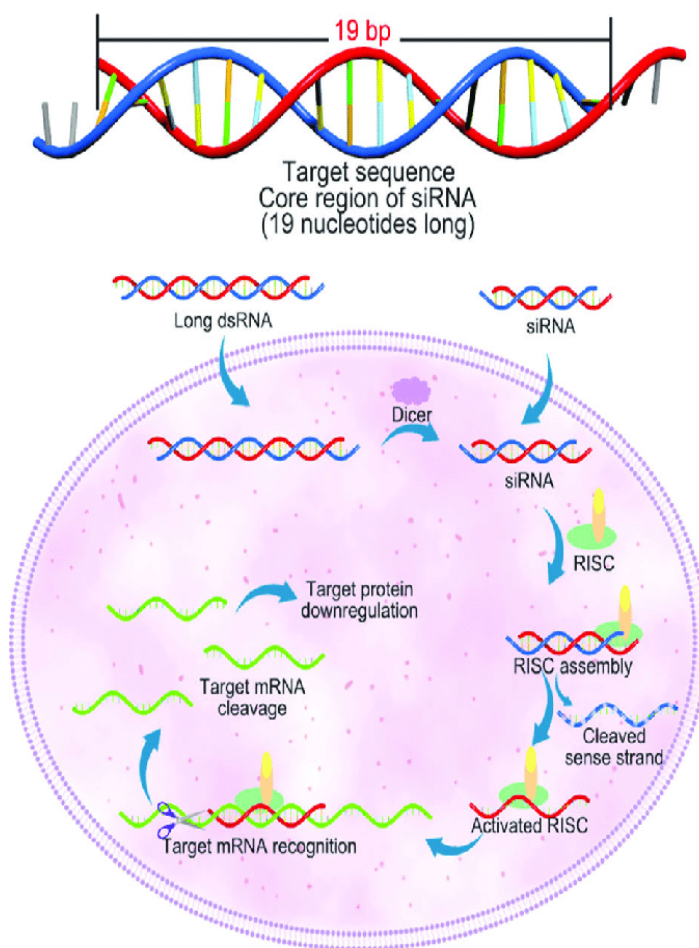
In the development of these siRNA-based therapies, the target binding could involve partial complementarity and induce multiple nonspecific effects, such as saturation of cellular proteins involved in the RNAi pathway. This off-target effect, for example, can stimulate the innate immune system and trigger an inflammatory response through the activation of Toll-like receptors. Based on this, Schlegel et al. (2013) developed siRNA-lipoplexes containing the anionic polymer polyglutamate aiming to reduce toxic effects induced by siRNA lipoplexes administered by systemic injection in mice. Compared to the cationic lipoplex, they observed that the anionic polymer addition induced an

extremely weak production of cytokines compared to the cationic lipoplex, which was not detectable after 24 h post-injection. Thus, it is essential to define the most specific siRNA sequence and safe delivery systems before their application *in vitro* or *in vivo*, using the lower concentrations as possible.

1.5 The eye as a therapeutic target for RNA interference

In the literature it is estimated that 285 million people are visually impaired in the world, suffering from ocular diseases such as age-related macular degeneration (AMD), diabetic retinopathy, uveitis, and glaucoma. Moreover, the number of patients suffering from chronic and progressive blinding retinal disorders is increasing due to the aging population. Currently, an effective clinical functional recovery of the retinal degenerative process has not been achieved and remains a major challenge (PASCOLINI and MARIOTTI, 2012; HUANG, CHEN and RUPENTHAL, 2018). Therefore, new therapeutic strategies are required to overcome physiological eye barriers and achieve intraocular therapeutic effectiveness. The advancement of RNAi design principles and delivery systems strongly suggests that targeted manipulation of gene expression via siRNA can be a promising technique to improve therapeutic outcomes in ophthalmic applications (THAKUR et al., 2012; SARETT et al., 2015; OLIVEIRA, ROSA DA COSTA and SILVA, 2017). Thus, this review will focus on significant advantages and limitations of retinal delivery of siRNA and the recent progress toward overcoming the natural ocular barriers.

The eye shows many advantages for RNAi therapies because it is easily accessible, relatively immune-privileged (due to the limited systemic exposure promoted by the blood-retinal barrier) and has small size, which makes it possible to obtain a therapeutic effect with low amounts of drug (WANG, RAJALA and RAJALA, 2015; PETIT, KHANNA and PUNZO, 2016; SARAIVA et al., 2017). The monogenic nature of retinal diseases and the recent knowledge of their molecular pathogenesis also contribute to the genetic pharmacology applications. Until now, more than 260 genes and loci related to the retinal diseases, such as RPE65-Leber congenital amaurosis (RPE65-LCA) and X-

linked juvenile retinoschisis were mapped in genetic basis (http://www.sph.uth.tmc.edu/RetNet/) (ADIJANTO and NAASH, 2015; OLIVEIRA, ROSA DA COSTA and SILVA, 2017). Furthermore, the majority of ocular diseases are bilaterally symmetrical, and the contralateral eye can be used as a control for the animal models (ROSSMILLER, RYALS and LEWIN, 2015; PETIT, KHANNA and PUNZO, 2016).

Despite the several characteristics of the eye that impulse the development as a genetic therapeutic target, the effectiveness of retinal treatment significantly depends on the siRNA vector ability to overcome the intraocular barriers. The delivery of therapeutic agents to specific ocular tissues is limited by a number of inherent anatomical and physiological ocular structures, including the cornea and anterior segment barriers, the sclera and Bruch's-choroid complex as well as the blood-retinal barrier (BRB) (DEL AMO et al., 2017; HUANG, CHEN and RUPENTHAL, 2018). For example, the vitreous humor can directly affect siRNA delivery to the retina due to its structure and composition. The anionic nature of vitreous can bind most of the cationic non-viral vectors and change the charge or size of the systems, decreasing their cellular uptake or intracellular release of the acid nucleic. Thus, the mobilization of these nanocarriers can be reduced because vitreous humor act as a molecular sieve and the nonviral gene complexes can be stick to collagen fibrils (PEETERS et al., 2005; MARTENS et al., 2015).

Moreover, the ocular administration route should be correctly selected (SOLINÍS et al., 2015; OLIVEIRA, ROSA DA COSTA and SILVA, 2017). The most used route of administration to the treatment of ocular diseases is the topical application. Direct instillation of siRNA aiming the treatment of ocular surface and anterior segment disorders *in vivo* has been investigated (CROOKE et al., 2009; MARTIN-GIL et al., 2012; GUZMAN-ARANGUEZ, LOMA and PINTOR, 2013). Nevertheless, when the target is the retina, it is well known that less than 5% of the drugs can reach retinal tissues after topical application, mainly because of limited diffusion through the sclera and the natural ocular barriers (DALKARA and SAHEL, 2014). Considering the

bioavailability of nucleic acids in the posterior segment of the eye after topical instillation, it is very low, mainly because of their size (BLOQUEL et al., 2006; SOLINÍS et al., 2015). Systemic administration shows similar results and only 1–2% of the therapeutic molecules administered can reach the vitreous cavity because of the existence of the BRB (THAKUR et al., 2012; OLIVEIRA, ROSA DA COSTA, and SILVA, 2017). Also, retinal delivery systems could be accomplished using other routes such as periocular (sub-conjunctival, sub-Tenon's, posterior juxtascleral, peribulbar, and retrobulbar injections) and suprachoroidal. However, these approaches may not result in adequate drug concentrations in the retina with currently available technologies (DEL AMO et al., 2017).

In this context, the most efficient method for targeted delivery of siRNA molecules to the posterior segment of the eye is the intraocular injection (HUANG and CHAU, 2019). Recent studies have used two types of injections to deliver siRNA nanocarriers to the retinal cells: subretinal and intravitreal (HERRERO-VANRELL, 2011; THAKUR et al., 2012; DALKARA and SAHEL, 2014). Subretinal injections of these delivery systems can provide the direct contact of the nucleic acids with photoreceptors, outer retinal layers, and RPE cells. Nevertheless, subretinal injections are technically more difficult than intravitreal and require the expertise of vitreoretinal surgeons, limiting its application on a large scale. For example, this procedure should detach photoreceptors from their supporting epithelium, creating a dome-shape bleb where therapeutic substances can be injected. In reason of the local retinal-detachment induced during the injection, photoreceptor cell death can occur and leads to a visual function loss (ZULLIGER, CONLEY, and NAASH, 2015; MARTENS et al., 2017). The other method, intravitreal injection, is an attractive tool to overcome the different natural barriers of the eye and expose the retina in contact directly with the siRNA vectors. In contrast to subretinal injection, it may be most clinically acceptable as an ocular route because it is simpler, less invasive and allows an introduction of higher molecules and drug doses. Even though intravitreal injections have been related with increased ocular pressure (IOP) and a small risk of endophthalmitis, these possible post-injection complications can be easily managed and cannot be compared to the risks of other intraocular administration routes

(ISSA and MACLAREN, 2011; ENGLANDER et al., 2013). As described before, the diffusion of the therapeutic agent to the photoreceptors and RPE must be evaluated as it can be reduced by significant physical barriers, such as the vitreous, the inner limiting membrane, and the inner retina with tightly filled extracellular matrix and cells (PEETERS et al., 2005). Since the exogenous genetic material can be efficiently internalized in the RPE, the phagocytic nature of this epithelium makes it a promisor target for gene delivery and most of the nucleic acids vectors have transduced the RPE with a high degree of efficacy (OLIVEIRA, ROSA DA COSTA and SILVA, 2017).

Figure 04 – Intravitreal and subretinal injections to reach the posterior segment of the eye.
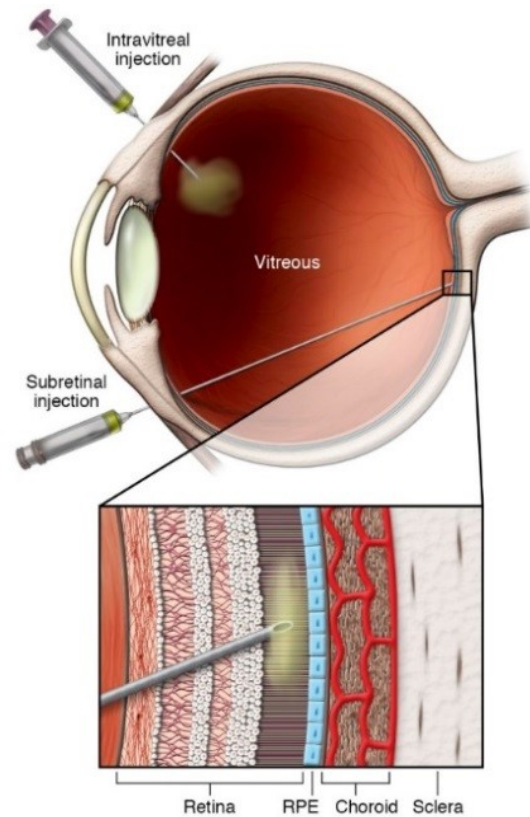
DICARLO, J. E; MAHAJAN, V. B; TSANG, S. H. Gene therapy and genome surgery in the retina. The **Journal of Clinical Investigation**, v. 128, n.6, p. 2177-2188, 2018.

1.6. siRNA delivery systems

The effectiveness of RNAi significantly depends on the siRNA vector ability to overcome intraocular barriers and reach the target cells. Currently, there are two main approaches used to facilitate the delivery of nucleic acids to the retina: viral vectors and non-viral vectors (MITRA, ZHENG, and HAN, 2015; DIAS et al., 2018). The most used viral vectors are those derived from adenoviruses, lentiviruses, and adeno-associated viruses, which can infect and transduce non-dividing cells, such as photoreceptors and RPE (DALKARA and SAHEL, 2014; SARAIVA et al., 2017). While many clinical trials successes have been achieved using viral vectors, they carry the risk of oncogenicity and immunogenicity. Based on this, there is an increasing interest in developing non-viral methods for a safe and efficient siRNA delivery system (YU-WAI-MAN et al., 2016; XIA, TIAN and CHEN, 2016).

1.6.1 Lipid-Based Liposomes Vehicles

In 1965, Bangham and co-workers published the first description of swollen phospholipid systems that became the basis for model membrane systems (BANGHAM et al., 1965). These authors showed that the phospholipids form hollow vesicles with a phospholipid bilayer where the lipophilic tails heading inside the lipid bilayer and the polar heads are oriented towards the interior and exterior aqueous phases. In the next few years, Gregory Gregoriadis (1973) was the first to establish the concept that liposomes could be used as drug carriers, suggesting that the elimination time from the blood for liposome-entrapped drugs was longer than for non-entrapped drugs (GREGORIADIS, 1973). After this, the pioneering work of several liposome researchers over more than five decades led to significant advances in the treatment of cancer, infections and genetic diseases (ALLEN and CULLIS, 2013; ZYLBERBERG and MATOSEVIC, 2016).

Liposomes are defined as self-forming lipid vesicles consisting of one or more concentric spheres of lipid bilayers, separated by water or aqueous buffer compartments (**Figure 05**). These particles are mainly composed of phospholipids such as phosphatidylcholine

(PC), phosphatidylethanolamine (PE), phosphatidylserine and phosphatidylglycerol. Due to their amphiphilic structure, liposomes can entrap lipophilic agents in the lipid membrane and hydrophilic agents in the aqueous core. Moreover, various ratios of natural or synthetic lipids could be used in liposome preparation to modulate the release profiles of encapsulated therapeutic molecules in the targeted tissue. The cholesterol, for example, is often added to liposomes formulations to stabilize the lipid bilayers and improve their properties as drug delivery systems (ALLEN and CULLIS, 2013; PATTINI et al., 2015).

Many factors influence the liposomal vesicle properties as the method of preparation, composition, size and surface charge. The preparation procedure is adapted to the substance that will be encapsulated, using methods such as the thin-film hydration or reverse phase evaporation, which will be described with more details in the next section. Regarding the composition, the choice of bilayer components can determine the permeability and the charge of the bilayer. For example, the use of saturated phospholipids with long acyl chains as Dipalmitoylphosphatidylcholine (DPPC) will form a bilayer structure more rigid and impermeable than unsaturated phosphatidylcholine as egg phosphatidylcholine. In addition, according to the lipid selected for liposome preparation, these lipid vesicles could be negatively charged, neutral, or positively charged at a specific pH environment. The charge of the liposome plays an essential role in their activity and stability. The positive charge on the cationic liposome surface facilitates contact with the negatively charged cell membranes and consequently, their internalization into the cells. Moreover, charged liposomes prevent the aggregation in storage conditions due to their electrostatic repulsion. Finally, the size is an important parameter to evaluate the amount of drug encapsulated in the liposomes and their circulation half-life. According to their size and lamellarity, they can be classified in small unilamellar vesicles (SUVs, 20-100 nm), large unilamellar vesicles (LUVs, >100 nm), multilamellar vesicles (MLVs, >500 nm) and giant unilamellar vesicles (GUVs, >1000 nm) (AKBARZADEH et al., 2013; PATTNI et al., 2015), as shown in **Figure 05**:

Figure 05- Schematic representation of different liposomes based on size and lamellarity.
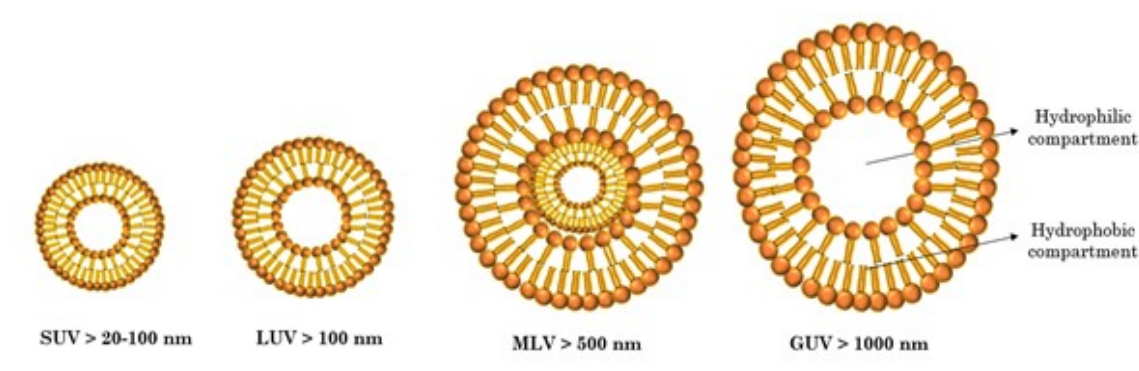
The several advantages provided by the use of liposomes as a drug-delivery system facilitate their transition from concept to clinical applications (WANG, RAJALA and RAJALA, 2015). Indeed, they are very appropriate for this aim due to the similarity with cell membranes, biocompatibility, biodegradability, and low toxicity. Moreover, the encapsulation of drug molecules or nucleic acids into the lipid bilayer can protect these agents on the journey to the target site, preventing enzymatic degradation or chemical inactivation. Nevertheless, some problems were observed during the *in vivo* studies of the first generation liposomes or conventional liposomes. The phospholipids have an intrinsic natural flip-flop or rotational freedom that difficult the retention of some types of entrapped molecules in liposomes interior. Further, the phospholipid membranes of conventional liposomes were strongly affected by physical interactions with circulating proteins in the blood (opsonization) and protein adsorption, which contributed to their rapid clearance after administration by the reticuloendothelial system (RES) (ALLEN and CULLIS, 2013). In order to overcome these problems, the second generation of liposomes was obtained by the inclusion of hydrophilic polymer shell as polyethylene glycol (PEG) on its surface. These new structures are called stealth liposomes, which displayed increased stability and prolonged circulation half-life compared to the conventional liposome (AKBARZADEH et al., 2013; ZYLBERBERG and MATOSEVIC, 2016). After this, other strategies involving the attachment of a targeting ligand at the surface of liposomes as antibodies or via fusogenic agents have also been explored.

For siRNA molecules that do not enter cells on their own, intracellular delivery is an essential requisite to trigger gene silencing. In particular, cationic liposomes have emerged as an interesting siRNA delivery vehicle owing to their electrostatic interaction with nucleic acids and potential high transfection efficiency into mammalian cells. Many commercially available cationic lipids, including Lipofectamine 2000, DOTAP (N-[1-(2,3-dioleoyloxy)propyl]-N,N,N-tri-methylammonium methylsulfate) and DOTMA (N-[1-(2,3-dioleyloxy) propyl]-N,N,N-trimethylammonium chloride), have been selected and applied to the delivery of nucleic acids (TAETZ et al., 2009; GASPERINI et al., 2015; ZYLBERBERG and MATOSEVIC, 2016).

1.6.2 Methods for the preparation of liposomes

There are a wide variety of methods that can be used to produce liposomal formulations. The choice of appropriate method is critical and depends on many parameters: 1) the liposome and the substance to be loaded physicochemical characteristics, toxicity, and concentrations; 2) the medium in which the liposomes are dispersed; 3) the conditions desired for their successful application such as the size, the half-life or additional processes during the delivery of the liposomes and 6) the costs and applicability regarding large-scale production for clinical purpose (BOZZUTO et al., 2015). The following is a brief description of conventional methods used in a research laboratory for liposome preparation, including Bangham, reverse-phase evaporation, detergent depletion, and solvent injection.

The thin-film hydration or Bangham method is one of the most widely used protocols for liposome-manufacture preparation (BANGHAM et al., 1965). This technique involves the dissolution of lipids in an organic solvent, followed by the evaporation of the organic solvent to form a lipid film. The final step is the dispersion of the lipid film in aqueous media. Although the Bangham method is one of the simplest methods for liposome preparation, the rehydration of this film produces large and nonhomogeneous MLVs that require sonication or extrusion processes to produce homogeneous small ULVs.

Moreover, it has limited use due to low aqueous core entrapment and the difficulty in removing the organic solvent (MEURE et al., 2008; AKBARZADEH et al., 2013).

An alternative method employed to obtain the liposomes is the reverse-phase evaporation (REV). This technique is carried out by dissolving the lipids in an organic solvent, adding a small volume of the aqueous phase and sonicating the solution to produce inverted micelles. First, a viscous gel forms while a rotary evaporator removes the organic solvent. Then, when sufficient solvent has been evaporated, the gel collapses and origins an aqueous suspension of MLVs. It is possible to encapsulate 30–45% of hydrophilic agents within REVs, reaching up to 65% entrapment at optimal conditions. However, this process is not recommended for the encapsulation of fragile molecules such as peptides, because of the high exposure to organic solvents (MEURE et al., 2008; BOZZUTO et al., 2015).

The detergent-depletion method is based on the formation of detergent-lipid micelles, followed by the removal of the detergent to obtain the liposomes. These micelles can be prepared by the hydration of a lipid film with a detergent solution or by drying both lipid and detergent from an organic solvent, then adding an aqueous solution. The detergent can be removed either by dialysis or size exclusion gel chromatography, which leads to the phospholipid's coalescence and production of LUVs. Compared to the other conventional techniques, a disadvantage of the detergent-depletion process is that the protocol used to remove the detergent may also remove any other small hydrophilic compounds. Moreover, this method is less used because its trapping efficiency is poor and time-consuming (MEURE et al., 2008; PATTNI et al., 2015).

Another technique described to obtain liposomes is the solvent injection method, which occurs by injection of phospholipids dissolved in an organic phase (ethanol or ether) into aqueous media. The ethanol injection method results in instant liposome formation after the solvent addition, but its application impairs the complete removal of the organic phase. On the other hand, the ether is immiscible with water, and its elimination is easier by heating during the formation of the liposomes. In this case, exposure to high

temperatures as well as the organic solvent may be detrimental to cargos. Both solvents used on injection methods described above result in the formation of heterogeneous vesicles of liposomes (PATTNI et al., 2015).

1.6.3 Cellular uptake of liposomes and endosomal escape

The study of the cellular uptake of liposomes has an important impact on their drug delivery efficiency. The endocytic pathways involved in nanocarriers uptake include micropinocytosis, clathrin-mediated, caveolae-mediated, and other clathrin- and caveolae-independent process (HILLAIREAU and COUVREUR, 2009; THAKUR et al., 2012). Like for other types of nanoparticles, the liposomes cell internalization will depend on their surface charge, size, cell type and the molecular composition of the cell surface. Thus, it is difficult to suggest a general consistent profile of liposomes uptake matching each of these endocytic pathways. Also, more than one endocytic mechanism can coincide (HILLAIREAU and COUVREUR, 2009). For example, lipid-based nanoparticles can be designed to be internalized through the clathrin-mediated pathway of endocytosis and metabolized into the lysosomes to release their content intracellularly. Other types of nanocarriers are tailored to by-pass the lysosomal degradation pathway and reach the cytoplasm via caveolin-mediated endocytosis, especially when the carried cargo is highly sensitive to enzymes (BAREFORD and SWAAN, 2007; THAKUR et al., 2012).

1.6.4 Lipoplex for an intravitreal application

When cationic liposomes are complexed with oligonucleotides, such as double-stranded DNA (dsDNA) and siRNA, this system is called a lipoplex. The overall charge and shape of lipoplexes are related to their lipid structure and conditional adjustments. Generally, the preparation of lipoplex involves the positive superficial charge for electrostatically bind the acid nucleic and helps it to interact with the cell surface, followed by the fusion with cell membrane and internalization into the endosomal compartment (NAYEROSSADAT, MAEDEH, and ALI, 2012; MITRA, ZHENG, and HAN, 2015; XIA et

al., 2016). However, this positive charge of the lipoplex can be detrimental for its intraocular mobility, inducing aggregation when they were exposed to the vitreal matrix (PEETERS, et al., 2007; MARTENS et al., 2015). Thus, for an intravitreal administration, it is essential to evaluate the superficial charge of the lipoplex to obtain a therapeutic efficacy in the retinal target cells (MARTENS et al., 2017). Recently, the new developments have focused on increase transfection efficiency and reduce cationic lipoplex cytotoxicity.

One of the strategies to improve the delivery of siRNA by cationic lipoplex is the association with Polyethyleneglycol (PEG). Although PEGylation of lipoplexes could prevent from aggregating in vitreous, this modification often showed lower transfection efficiency in retinal pigment epithelial cell line (JIN et al., 2014; OLIVEIRA, ROSA DA COSTA and SILVA, 2017). In 2011, Liu and collaborators investigated the use of the PEGylated liposome protamine-hyaluronic acid nanoparticles complexed with siRNA aiming the treatment of choroidal neovascularization (CNV) in rats. The authors concluded that these cationic PEGylated nanoparticles efficiently protect the siRNA and could facilitate the nuclei acid internalization into the cells, silencing VEGFR1 expression and reducting CNV area. However, they suggested that most of the lipid nanoparticles administered remained in the vitreous body and did not reach the retina (LIU et al., 2011). Some authors attributed this result to the fact that PEGylation can interfere on the cellular interactions and decrease uptake of lipoplexes (MISHRA, WEBSTER and DAVIS, 2004; SANDERS et al., 2007; PEETERS et al., 2007; MARTENS et al., 2017). In another study, Song et al. (2002) suggested that the incorporation of PEG-lipids stabilizes the lamellar phase of the lipoplexes and avoids the phase transition from the endosomal release (PEETERS et al., 2007; XIA et al. 2016). Many approaches have been proposed to overcome the drawbacks of PEGylation the lipoplexes. Wheeler et al. (1999) were the first authors to demonstrate that 'exchangeable' PEG–ceramides (with a short C14 acyl chain) can improve the efficiency of transfection of PEGylated lipoplexes, by increasing the contact with the cytoplasmic membranes of the target cells (WHEELER et al., 1999; PEETERS et al., 2007). In other study made by Shi and co-

workers, it was reported that PEG–ceramides with a short acyl chain enhanced the gene expression by promoting a better endosomal escape of the lipoplexes (SHI et al., 2012).

The association between cationic liposomes and hyaluronic acid (HA) is another method of targeting the retina. HA is a glycosaminoglycan composed of nonesterified disaccharide units of N-acetylglucosamine and glucuronic acid chains alternately $\beta1{\rightarrow}4$ and $\beta1{\rightarrow}3$ (WOJCICKI et al., 2012). This biopolymer composes the vitreous matrix and it has many physiological essential functions that include tissue and matrix water regulation, structural and space-filling properties, lubrication, mucoadhesion, and several macromolecular functions (WOJCICKI et al., 2012; MARTENS et al., 2015 and 2017).; MARTENS et al., 2015 and 2017). The conjugation of HA to the surface of liposomes can be done through two routes, the chemical derivatization of molecules to incorporate HA in the phospholipids and the coating of cationic liposome with HA. Liposome−HA chemical derivatization can be obtained by coupling HA molecules covalently to the polar headgroup of the lipid, using conventional procedures for liposome production. For example, the chemical conjugate HA−1,2-dioleoyl-sn-glycero-3-phosphoethanolamine (HA−DOPE) was used to prepare cationic liposomes to deliver the plasmid DNA pCMV-luciferase. In this study, lipoplexes containing HA-DOPE showed that 10% HA-DOPE (w/w) was optimal for the transfection of MDA-MB231 breast cancer cells expressing CD44 (TAETZ et al., 2009; SURACE et al., 2009; GASPERINI et al., 2015). In another study made by Wojcicki and collaborators (2012), the transfection efficiency on the CD44-expressing A549 lung cancer cells was determined by flow cytometry in the presence of 0, 10 and 15% of HA-DOPE or unconjugated HA. Lipoplexes at lipids: DNA ratio of 2 containing 10% (w/w) of HA-DOPE improved the transfection efficiency comparing to the other formulations tested (WOJCICKI et al., 2012).

The other way is to develop a surface-modified liposome using an electrostatic interaction between cationic liposomes and HA. In a study made by Sagristá et al. (2000), it was proved that HA-coated liposomes were able to encapsulate and hold drugs. Later on, Esposito and collaborators (2008) demonstrated the proof-of-concept

that cationic liposomes were successfully functionalized with HA (103−104 kDa) and loaded with a magnetic resonance imaging (MRI) contrast agent. These authors reported that the noncovalent binding between HA and liposomes was simple, resulting in efficient and specific MRI contrast agent with the cell-targeting ability and low toxicity. Also, the results showed the affinity between the HA−liposome complexes and the C6 cell line, which expresses high levels of the CD44 receptor (ESPOSITO, GENINATTI CRICH and AIME, 2008). Currently, to understand all the mechanisms of the cationic liposomes and HA complexation, systematic studies of the electrostatic interactions are needed. The formation of this complex can be considered a polymer-vesicle system in which mutual interactions such as electrostatic bridging, hydrophobic and hydrogen-bond interactions control the polymer-vesicle association or segregation. These studies could also be useful to a better understanding of polymer−vesicle associations aiming further *in vivo* or *in vitro* applications (GASPERINI et al., 2015).

In 2015, Martens and co-workers tested HA as an alternative coating to obtain optimal vitreal mobility with efficient retinal cell uptake. Using a previously optimized *ex vivo* model, this study confirmed that electrostatic coating of PEGylated lipoplexes using HA provides good mobility in bovine vitreous humor similar to the lipoplexes functionalized only with PEG, but with higher uptake in ARPE-19 cells (MARTENS et al., 2015). Later on, in 2017 these authors compared the electrostatic binding with the covalent binding of HA on the DOTAP: DOPE/plasmid DNA lipoplexes effect in terms of nanoparticle's vitreal mobility and gene transfection efficiency *in vitro*. Both systems resulted in anionic, monodisperse HA-lipoplexes and showed an improvement of intravitreal mobility compared to uncoated lipoplexes. According to Martens et al. (2017), while electrostatic coating provides an easy way of coating cationic nanoparticles, *in vitro* studies indicated that covalent binding showed higher increased transgene expression (MARTENS et al., 2017). However, the stability and internalization of these systems in retinal tissues *in vivo* was not investigated.

1.7 Electroretinography (ERG)

The electroretinography (ERG) is a widely used electrophysiologic test of retinal function (MARMOR et al., 2008). The visual acuity is measured by recording electrical activity upon luminous stimulation, based on changes in ion currents within the retina. The conventional ERG is a non-invasive and objective test useful clinically for input to the diagnosis of several retinal diseases. There are different types of ERGs – full-field ERG, pattern ERG and multifocal ERG. As retinal diseases characteristically change the ERG responses, it serves as a standard diagnostic tool in clinical ophthalmology and scientific research. Moreover, it is an optimal assay for translational research, considering that a similar methodology can be used in laboratory animals and humans (WEYMOUTH and VINGRYS, 2008; MIURA et al., 2009).

The International Society for Clinical Electrophysiology of Vision (ISCEV) establishes standard clinical protocols for electrophysiological examinations. During a general ERG exam, the flash of light can be modulated using different parameters and luminous sources stimulations to observe the functionality of distinct retinal cell classes. Single-flash ERGs provide essential information on the retinal functionality, mainly when they are recorded at a luminance series from low to high intensities, under both dark-adapted and light-adapted conditions. In this case, it is possible to evaluate the first, second and third-order neurons of the retina, as well as the rod and the cone photoreceptor pathways **(Figure 06)**. An ISCEV Standard flash ERG recommendations include the following responses, named according to conditions of adaptation and the stimulus (flash strength in $cd \cdot s \cdot m^{-2}$): (1) Dark-adapted 0.01 ERG (formerly "rod response"); (2) Dark-adapted 3.0 ERG (formerly "maximal or standard combined rod-cone response"); (3) Dark-adapted 3.0 oscillatory potentials (formerly "oscillatory potentials"); (4) Light-adapted 3.0 ERG (formerly "single-flash cone response"); (5) Light-adapted 3.0 flicker ERG (formerly "30 Hz flicker"). The five basic ERGs represent the minimum ERG evaluation for clinical diagnosis (MARMOR et al., 2008).

Figure 06 - ERG single-flash incidence and retinal cells response.
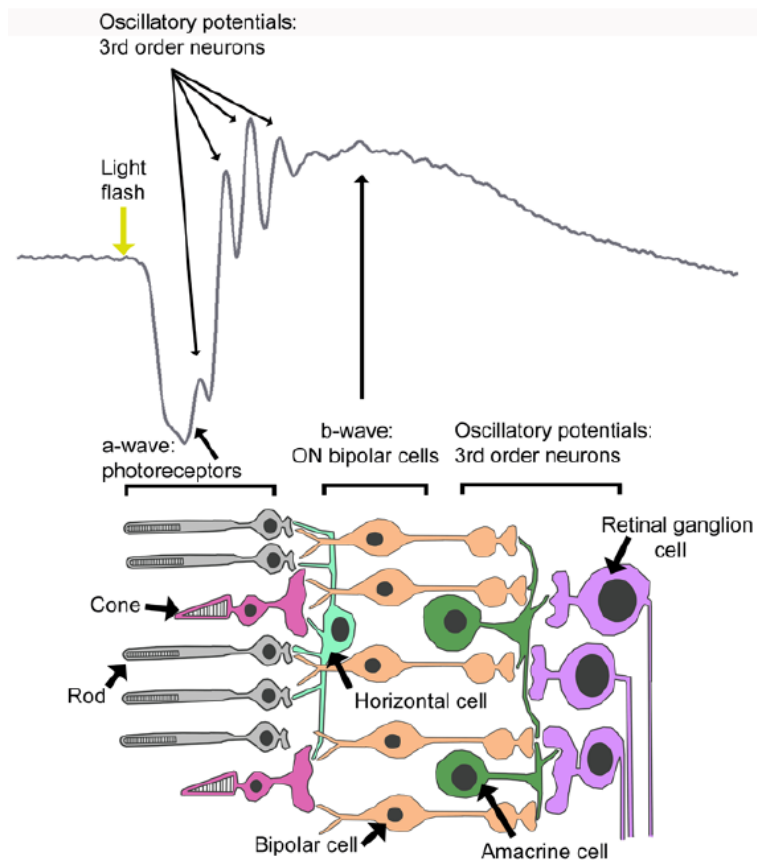
Oscillatory potentials:
3rd order neurons

Light
flash

a-wave:
photoreceptors

b-wave:
ON bipolar cells

Oscillatory potentials:
3rd order neurons

Retinal ganglion
cell

Cone

Rod

Horizontal cell

Bipolar cell

Amacrine cell

Moreover, the ideal flash stimulus for studying retinal physiology is one that shows the capacity for high luminous output over a short period, promoting a saturation of neuronal responses that have fast integration times. According to the ISCEV protocols, the light stimulus of duration used must be considerably shorter than the integration time of any photoreceptor, generally having a duration of 5 ms. Although these protocols have been well designed to identify human disease and disorders by using the ERG, their direct application to rodents and other species is limited. Therefore, specific guidelines for the isolation of rod and cone contributions from the full-field ERG in rodents are also published (WEYMOUTH and VINGRYS, 2008).

The rodent clinical ERG is generally represented by a biphasic waveform recordable from the cornea after the luminous stimulus, similar to that illustrated below **(Figure 07)**. Two components are most often measured in the experimental analysis of retinal functions: the a-wave (corneal-negative deflection) and the b-wave (corneal-positive) deflection. The a-wave is primarily driven by photoreceptor activation and the b-wave is mainly generated by predominantly Muller and ON-bipolar cells (LEINONEN and TANILA, 2017). ERG exam results can be analyzed using values assigned to implicit time, latency and amplitude of the a and b-waves. Implicit time is the time from the flash to the apex of the "a" wave, latency is the time between the flash and the beginning of the wave, and amplitude is the distance from the base to the apex of the wave. Additionally, there are the oscillatory potentials (OPs) that frequently appear as high-frequency wavelets superimposed on the b-wave of the ERG. The OPs profile depends on the intensity, rate and spectral characteristics of the light stimulus, showing a better recorder condition after an intense white light flash. The cellular origin of these potentials remains controversial, but it is generally accepted that they reflect third-order neural events such as activation of amacrine and/or ganglion cells (YU and PEACHEY, 2007; CAMERON et al., 2008). Together these elements represent an important tool to study the majority of retinal functions.

Many factors should be considered and controlled to avoid external interferences in the ERG measurements, such as pupillary dilatation, anesthesia, ambient temperature, equipment, type, intensity and wavelength of the light stimulus. In rodent exams, the animal's head is positioned in the center of the Ganzfeld dome, which disperses the light homogenously and the flash of light reaches the whole retina approximately uniformly. Also, it is crucial to choose the animal protocol according to the goal of visual analyses. For example, while to investigate rod-mediated vision is used a dark-adapted state, to extract cone-driven responses it is necessary to submit the animal to a light-adaptation state (LEINONEN and TANILA, 2017)

Figure 07 - Measurement of the a-wave and b-waves from a dark-adapted ERG. The trace shown is recorded from the cornea of a rodent with a dark-adapted eye, after a bright flash of light given at the time shown t0. The a-wave amplitude is measured from the baseline to the first trough (red arrow). For the b-wave amplitude, it is measured from the trough of the a-wave to the following positive peak (blue arrow).
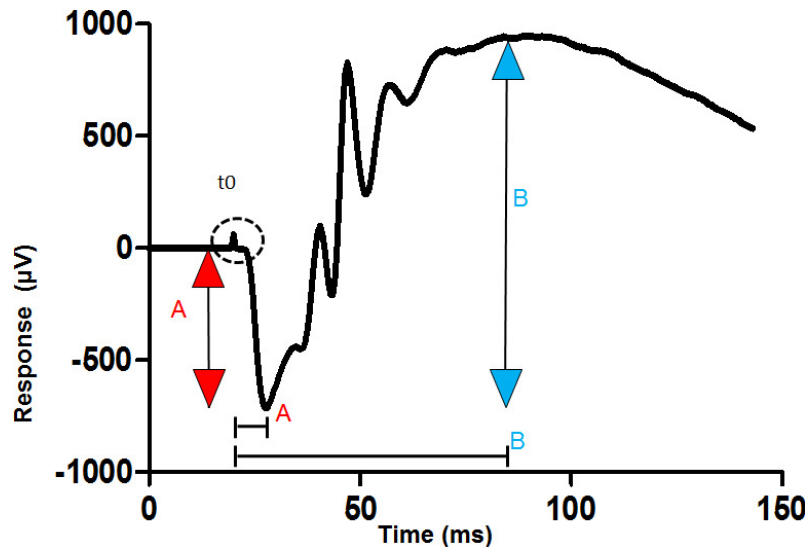
BRANDLI A, STONE J. Using the Electroretinogram to Assess Function in the Rodent Retina and the Protective Effects of Remote Limb Ischemic Preconditioning. **Journal of Visualized Experiments,** v. 100, p.1-8, 2015.

For recording the retinal signals, several types of electrodes are used such as contact lenses with conductive metal electrodes embedded in them, thin fibers with silver particles or gold foil electrodes. The recording electrode must provide good ocular contact and reproducibility, to ensure that waveforms are comparable to standard ERGs, and to define both normal values and variability (MARMOR et al., 2008). These electrodes are generally placed on the corneal surface of anesthetized animals and a lubricating ionic conductive solution is used to protect the eyes (FRISHMAN and WANG, 2011). Moreover, this solution must be a non-irritating and non-allergenic solution that is relatively non-viscous (i.e., no more viscous than 0.5% methylcellulose), since more viscous solutions can attenuate signal amplitude (MARMOR et al., 2008). Reference and ground electrodes are also used. The signal response to a high-intensity stimulus is generally peak to peak, from a microvolt or less up to a millivolt or even more. Then, all the signals obtained with the electrodes are amplified using conventional

electrophysiological amplifiers, because ERG signals in mammals are small. Amplifiers and digital filter settings in the software are important for keeping relevant signals and eliminate others out of the frequency range, for example, a low-frequency drift of line noise (FRISHMAN and WANG, 2011).

2. CHAPTER 02: Experimental work

Development and characterization of lipoplex covered by hyaluronic acid for siRNA delivery to retinal cells

2.1 INTRODUCTION

RNA interference (RNAi) has recently advanced as a powerful tool to achieve highly specific gene regulation. In this process, the most common molecules used to downregulate the gene of interest expression by driving the target messenger RNA to degradation are the small interfering RNAs (siRNAs). siRNA is a double-stranded RNA oligonucleotide of 19-21 base pairs that offer the possibility of a selective and long-lasting therapeutic effect for gene-related diseases. Although this technique can specifically silence the expression of any chosen gene, different barriers to the intracellular delivery of siRNA significantly limit its clinical efficacy. The delivery of naked siRNA molecules is unlikely to be effective because they cannot freely cross cell membranes due to their relatively broad molecular weight and phosphodiester backbone. In addition, there are endonucleases and exonucleases that can rapidly degrade siRNA. Thus, new delivery systems are needed to facilitate the internalization of siRNA into cells and also to avoid its degradation by RNases (HAMOUDI et al., 2015; YU-WAI-MAN et al., 2016; ARRUDA et al. 2019).

Regarding an ocular application, lipid-based liposomes are the most studied nonviral delivery vectors for the treatment of many retinal diseases (WANG, RAJALA and RAJALA, 2015; DELPLACE, 2015; OLIVEIRA, ROSA DA COSTA and SILVA, 2017). Generally, lipoplexes are formed by spontaneous binding of nucleic acids to cationic liposomes, as these nanoparticles can protect siRNA from degradation and also facilitate its endocytosis in target cells. However, the positive charge of cationic lipoplex can be detrimental for its mobility and induce aggregation into the vitreous (PEETERS, et al., 2007; MARTENS et al., 2015). In this context, one promising alternative of targeting the retina is coating cationic liposomes with an anionic polymer such as hyaluronic acid (HA). HA has good biocompatibility, biodegradability and it is naturally present in the eye as a major constituent of the extracellular matrix of vitreous humor (WOJCICKI et al., 2012; KOO et al., 2012; GASPERINI et al., 2015). Moreover, this biopolymer plays an important role in cell signaling and can bind cell membranes via

CD44 receptors, expressed on the surface of hematopoietic, neuronal and epithelial cells (HUANG and HUANG, 2018).

In the present study, cationic lipoplexes were functionalized with HA for enhanced siRNA transfer and intraocular stability. Optimization of lipoplex coating was tested using two different molecular weights of HA (8-15 kDa and 160-600 kDa). The optimized formulation was successful in facilitating cellular uptake of siRNA and show higher transfection efficiencies than cationic lipoplexes formulated using Lipofectamine®. Also, HA-lipoplex were not cytotoxic to ARPE-19 cells at siRNA concentration used in transfection assays. These results made the HA-lipoplex an attractive nanoparticle to deliver therapeutic siRNA to retinal cells and a promising system for *in vivo* studies.

2.2 MATERIAL AND METHODS

2.2.1 siRNAs and plasmids

siRNA (5' UUC UCC GAA CGU GUC ACG UdTdT 3') and Rhodamine-labelled siRNA were purchased from Eurogentec. Plasmid pAd-RFP was obtained from Addgene.

2.2.2 Liposomes and lipoplexes

Cationic liposomes were prepared as reported previously by our research group composed by DMAPAP cationic lipid (RPR 209120 2-{3-[Bis-(3-amino-propyl)-amino]-propylamino}-N-ditetradecyl carbamoyl methyl-acetamide, synthesized as in BYK et al., 2001) and DOPE (1,2-dioleoyl-sn-glycero-3-phosphoethanolamine) obtained from Avanti Polar Lipids (RHINN et al., 2009; HAMOUDI et al., 2015). First, to obtain the liposomes, a chloroformic solution of an equimolar mixture of DMAPAP and DOPE is prepared. Then, the organic solvent is evaporated under vacuum to form a thin lipid film, using a rotary vacuum evaporator at 20 °C. After this process, this lipid film is rehydrated to produce large multilamellar vesicles and sonicated (115 V, 80 W, 50–60 Hz) with a G112SP1G model sonicator (Laboratory Supplies Co. Hicksville, N.Y.) to obtain a homogeneous suspension of liposomes.

Lipoplexes were prepared by mixing a siRNA (1.5 µg) or pAd-RFP plasmid (1.5 µg) and sodium alginate solution (Sigma-Aldrich) at ratio 1:1 (w/w) in 150 µL of NaCl 150 mM, with an equal volume of the cationic liposome suspension also prepared in 150 mM NaCl. Lipoplexes were allowed to form for 30 minutes at room temperature before use. The charge ratio of cationic lipoplexes was R+/-=8, calculated using the molar ratio of positive charges (positive charges per molecule of DMAPAP) to the molar ratio of negative charges (from siRNA and anionic polymer molecules, respectively siRNA 3.03 and AA 5.05 nmoles of negative charges/mg).

For coating lipoplex with hyaluronic acid, the cationic lipoplexes were rapidly mixed by vortexing with an equal volume of hyaluronic acid solution 0.3 % (w/v). We tested two different molecular sizes of HA aiming lipoplex surface-modification: 160-600 kDa (Bio-sodium hyaluronate powder) and 8-15 kDa (Sodium hyaluronate Contipro).

2.2.3 Dynamic Light Scattering (DLS) and Zeta Potential

Hydrodynamic diameter (intensity- weighted Z-average), polydispersity index (PDI) and zeta potential (ZP) of cationic lipoplex and HA-lipoplex were measured by dynamic light scattering with a NanoZS Zetasizer (Malvern Instruments).

2.2.4 Transmission Electron Microscopy (TEM) and cryo-TEM

For TEM, samples preparation of different types of lipoplex were performed as follows: 3μL of each formulation was placed on 400 mesh coated copper grids (Lacey Formvar/Carbon, EMS) allowed to adsorb and the excess amount of liquid was removed with a filter paper. Negative staining was made with uranyl acetate and preparations were analyzed at room temperature on a Tecnai Spirit 120 electron microscope operating at an accelerating voltage of 120 kV under low electron dose.

For cryo-TEM analysis, cryo-TEM grids were prepared using a Plunge freezing GPM2 (Leica). Specimens were prepared in a controlled environment with the temperature and humidity set to 22 °C and 100%, respectively, which prevented sample evaporation during the preparation. A 3 μL sample droplet was deposited on a 400 mesh lacey carbon-coated cooper grid (EMS) and prepared with a blot time of 3 s. Specimens were analyzed in low dose condition, on a Tecnai Spirit 120 electron microscope operating at an accelerating voltage of 120 kV.

2.2.5 Electrophoresis

For this assay, uncoated lipoplexes and lipoplex covered by hyaluronic acid were prepared in 150 mM NaCl containing 0.3 µg siRNA/sample (in 10 µL). The same concentration of naked double-stranded siRNAs was used as control. To release the nucleic acid from the nanoparticle structures, the samples were treated with NaCl 1 M solution and 10% Triton X 100 (Sigma-Aldrich) at 25 ºC for 20 minutes. Afterward, 10 µL of TBE-urea sample buffer 2× was added to the samples and they were electrophoresed on 8% polyacrylamide gels in TBE buffer running at 90 V for 40 minutes. After migration, the gel was stained with ethidium bromide for 30 minutes. Then, the stained siRNA bands were visualized under UV transilluminator.

2.2.6 Cell culture

The ARPE-19, a human retinal pigment epithelial cell line, was cultured in Dulbecco's Modified Eagle Medium: Nutrient Mixture F-12 (DMEM/F-12, Life Technologies) supplemented with 2.43 g/L sodium bicarbonate (Sigma-Aldrich), 1 % penicillin/streptomycin/amphotericin B solution (PSA; Sigma-Aldrich) and 10% Fetal Bovine Serum (Gibco). Cells were cultivated in a humid atmosphere at 37 °C, 5% CO_2. The culture media was changed every 2 days.

2.2.7 Detection of CD44 expression on ARPE-19 cells

ARPE-19 cells were seeded in 96-well plates at 1×10^4 cells/well and allowed to grow overnight. The next day, the cells were washed with PBS and fixed with paraformaldehyde 4%(w/v). The cells were blocked with BSA 1% for 1 h and incubated overnight with a primary anti-CD44 antibody (rabbit, Abcam). The negative control was included by omitting primary antibodies. After washing, a green fluorescent bovine secondary anti-rabbit Alexa 488 antibody (Thermo Scientific) was added to the cells and incubated for 30 minutes in the dark. Afterward, the cells were washed and the nuclei

marked with DAPI (Life Technologies). The CD44 expression was evaluated using the Zeiss LSM 880 (Carl Zeiss) confocal microscope.

2.2.8 HA-lipoplex cytotoxicity

Cytotoxicity was evaluated by the colorimetric method MTT. Briefly, the cell suspension was seeded on 24-well plates at the density of 1 x 105 cells/well with HA-lipoplex containing 2 different concentrations of siRNA (37.6 uM and 75.4 uM), added to the cells in triplicate. Next, the cells were incubated at 37 °C in the presence of 5% CO_2 for 24 h. Then, the medium containing the lipoplexes was replaced by a fresh culture medium and the cells were incubated for an additional period until 48 h. The viability was evaluated adding MTT (0.5 mg dissolved in 1ml of DMEM) directly into the cell plates and incubated for 5 h, when the viable cells convert the MTT to formazan crystals. In sequence, these crystals were suspended using a solution of isopropanol containing 0.06 M HCl and 0.5% SDS. The color intensity of the samples was measured spectrophotometrically in a microplate reader at 570 nm and results were expressed relative to untreated cells.

2.2.9 Uptake of HA-coated lipoplex in ARPE-19 cells

ARPE-19 cells were plated onto 6-well plates containing sterile glass slides at 1 x 10^5 cells/well, in 2 mL of culture medium added with lipoplex formulation. Lipoplexes coated with hyaluronic acid were prepared as described above using control siRNA (without fluorescence) or Rhodamine-labelled siRNA. For the positive control, Lipofectamine® 2000 (Thermo Fisher Scientific) containing the same concentration of Rhodamine-labelled siRNA incorporated in lipoplexes was used. Twenty-four hours after plating, cells were washed with PBS and fixed for 10 min with 10% (w/v) paraformaldehyde. Then, these cells were incubated in presence of PBS containing 0.1 % Triton X-100 (Sigma-Aldrich) for 5 min and blocked in PBS 1% (w/v) Bovine Serum Albumin (BSA, Sigma-Aldrich) and PBS 5% goat serum. In addition, the cells were double-labeled with monoclonal antibodies against α-tubulin (Sigma-Aldrich) and lamin B1 (Abcam). Next,

cells were washed with PBS and incubated with secondary antibodies conjugated to Alexa 488 and 647 plus the nuclear stain Hoechst 33258 (Life Technologies). Cells were washed in PBS and mounted in Prolong Gold Antifade reagent (Life Technologies). The negative control was included by omitting primary antibodies. The Zeiss LSM 880 (Carl Zeiss) confocal microscope was used to obtain the images with an oil 63X 1.4 NA objective lens with excitation at 405, 488, 543 and 633 nm. The ZEN Black edition software (Carl Zeiss) was used to process the images

2.2.3 Transfection

The reverse transfection procedure was used to transfect Rhodamine-labelled siRNA or pAd-RFP into ARPE-19 cells. The HA-lipoplexes were prepared with siRNA as described above or with a plasmid (1 ug/uL). Lipofectamine® 2000 (Thermo Fisher) was used as a reference and prepared according to the manufacturer recommendations, containing the same concentration of siRNA or pAd-RFP used in HA-lipoplexes. First, these formulations were added into 24-well culture plates. In sequence, cells were seeded on the wells at 1×10^5 cells/well. The transfection medium used was a reduced serum medium Opti-MEM^{tm} (Gibco). ARPE-19 cells were incubated with the gene transfer materials for 24 h at 37 °C in the presence of 5% CO_2. Then, the transfection medium was replaced by a fresh culture medium and the cells were incubated for an additional period of 24 h at 37 °C. Finally, the transfected cells were washed with PBS and lysed with 200 µl cell culture lysis reagent (Promega). To obtain the main fluorescence intensity, each well was measured by Cytation 5 Cell Imaging Multi-Mode Reader (Bio Tek Instruments) and the software Gen5 (Bio Tek) with a fixed gain, λ_{ex} =550-570 nm and λ_{em} = 600-620 nm. The transfection efficiency was expressed as the main relative fluorescence unit (RFU) values of each sample. The Pierce BCA assay (Thermo Scientific) was used to normalize the protein concentration of the samples. All the experiments were performed in triplicate for each sample.

2.3.4 Data analysis

The statistical analyses were performed using GraphPad PrismTM software. All the data were expressed as mean ± standard deviation (SD) and statistical differences were analyzed using one-way analysis of variance (ANOVA) and post-test of Bonferroni. Results with $p < 0.05$ were considered significant.

2.3 RESULTS

2.3.1 Physicochemical and morphological characterization of lipoplexes

To modify the surface of liposomal siRNA delivery systems, we have taken advantage of the possibility of establishing an electrostatic interaction between HA and cationic lipoplexes. We have tested two different molecular sizes of HA: 160-600 kDa and 8-15 kDa, prepared as 0.3 % (w/v) solution and mixed with siRNA lipoplexes. The obtained nanoparticles were characterized in terms of mean diameter, polydispersity index (PDI) and zeta potential (**Table 1**). Uncoated lipoplexes showed the size and zeta potential of 133.5 ± 1.2 and + 71.1 ± 3.0 mV, respectively. HA-lipoplexes prepared with HA of low molecular weight (8-15 kDa), presented visible flocculation in suspension during the coating process. Therefore, the size could not be measured. In contrast, with HA of higher molecular weight (160-600 kDa), a monodisperse nanoparticle suspension with an anionic surface charge was obtained. The mean size increased at about 66% compared with uncoated lipoplex and surface potential decreased from 71.1 ± 3.0 mV to -34.2 ± 1.4 mV. These results were reproducible and indicated an electrostatic binding between HA and lipoplexes. Hereafter, in this study, only sodium hyaluronate with a molecular weight of 160 to 600 kDa was used to prepare HA-lipoplexes.

Table 01- Size, PDI and zeta potential of lipoplex in NaCl 150 mM, as measured by dynamic light scattering.

	Z-averaged diameter (nm)	Pdl*	Zeta potential (mV)
Uncoated lipoplex	133.5 ± 1.2	0.217 ± 0.014	71.1 ± 3.0
Lipoplex HA (8-15 kDa)	p	p	-6.0 ±1.3
Lipoplex HA (160-600 kDa)	221.8 ± 9.2	0.220 ± 0.068	-34.2 ± 1.4

*PDI: Polydispersive index
p: visible precipitates in the sample

Next, the lipoplex morphology was analyzed before and after the HA coating by two different techniques, TEM and cryo-TEM. Spherical morphologies showing multiple lipid bilayers were found for both lipoplex formulations, but cationic showed more LUVs while HA-lipoplex showed more MLVs. In general, the vesicles of lipoplex were found attached to each other, but with a well-defined interface. The irregular core of cationic lipoplex (**Figure 01, IA**) is probably due to the sample preparation before the TEM analyses.

Figure 01- TEM images (A) and Cryo-TEM images (B) of cationic lipoplex (I) and HA-lipoplex (II). Scale bar:100 nm.
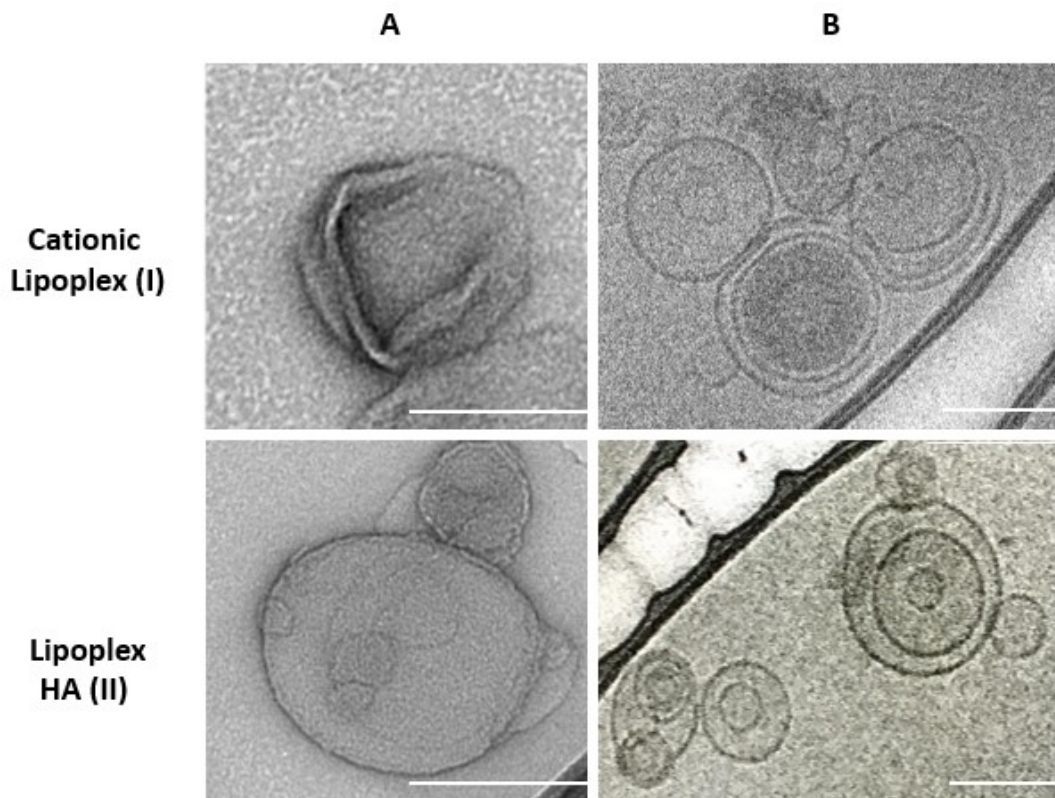
2.3.2 Electrophoresis

Assessment of the siRNA complexation with uncoated or HA-lipoplexes was done by electrophoresis on acrylamide gel, **Figure 02**. For this, naked double-stranded siRNA bands were compared with the siRNA bands released from these nanoparticles after they were prepared. Lipoplex samples (**Figure 02, band 03-06**) were treated with Triton X-100 and NaCl 1M for 20 minutes to release siRNAs by solubilization of the lipids and subsequent dissociation of these complexes. One sample of naked siRNA also received this treatment to compare with lipoplexes in the same conditions. According to the results, both lipoplexes were able to complex with siRNA and maintain the acid nucleic binding in these experimental conditions when the treatment was not added (**Figure 02, band 03 and band 05**). In addition, comparing the siRNA released band from uncoated lipoplex (**Figure 02, band 04**) and HA-lipoplex (**Figure 02, band 06**), even observing a little difference in their profile, their electrophoretic migration and amount were comparable to the naked siRNA band migration. Based on this, we can suggest that the HA coating did not affect the incorporation and release of siRNA from the nanoparticles.

Figure 02. Acrylamide gel electrophoresis analysis of naked siRNA and lipoplexes, covered or not with hyaluronic acid. Each sample contains 0.3 µg of siRNA, electrophoresed through 8% acrylamide gel at 90 V for 40 minutes. (1) Band of intact naked double-stranded siRNA; (2) naked double-stranded siRNA after the treatment with Triton X-100 and NaCl 1 M solution; (3) siRNA complexed in the cationic lipoplex without treatment; (4) Band of siRNA released from uncoated lipoplex, after the treatment for dissociation of these particles; (5) siRNA complexed in the HA-lipoplex without treatment; (6) Band of siRNA released from HA-lipoplex, after the treatment for dissociation of these particles.
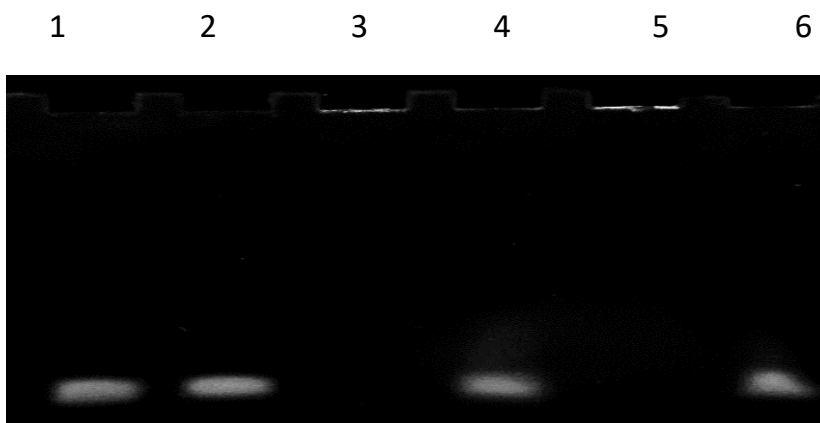
2.3.3 Detection of CD44 expression on ARPE-19 cells

CD44 is the main transmembrane adhesion receptor for HA. As we expect that HA-lipoplex will internalize by association with the CD44 receptor, we investigated its expression levels on the surface of ARPE-19 via immunofluorescence staining with antibodies to CD44 receptors. In **Figure 03**, it was possible to verify a high expression of CD44 and also clustering on the cytosol of retinal cells. A fluorescent signal was not observed in negative control cells that were incubated without these primary antibodies.

Figure 03. CD44 expression in ARPE-19 cells evaluated by immunofluorescence. (1) Negative control: cells incubated without primary antibodies. (2) Cells stained with antibodies directed against CD44 (green). The nuclear stain was made with DAPI. Representative images were taken by confocal laser microscopy.
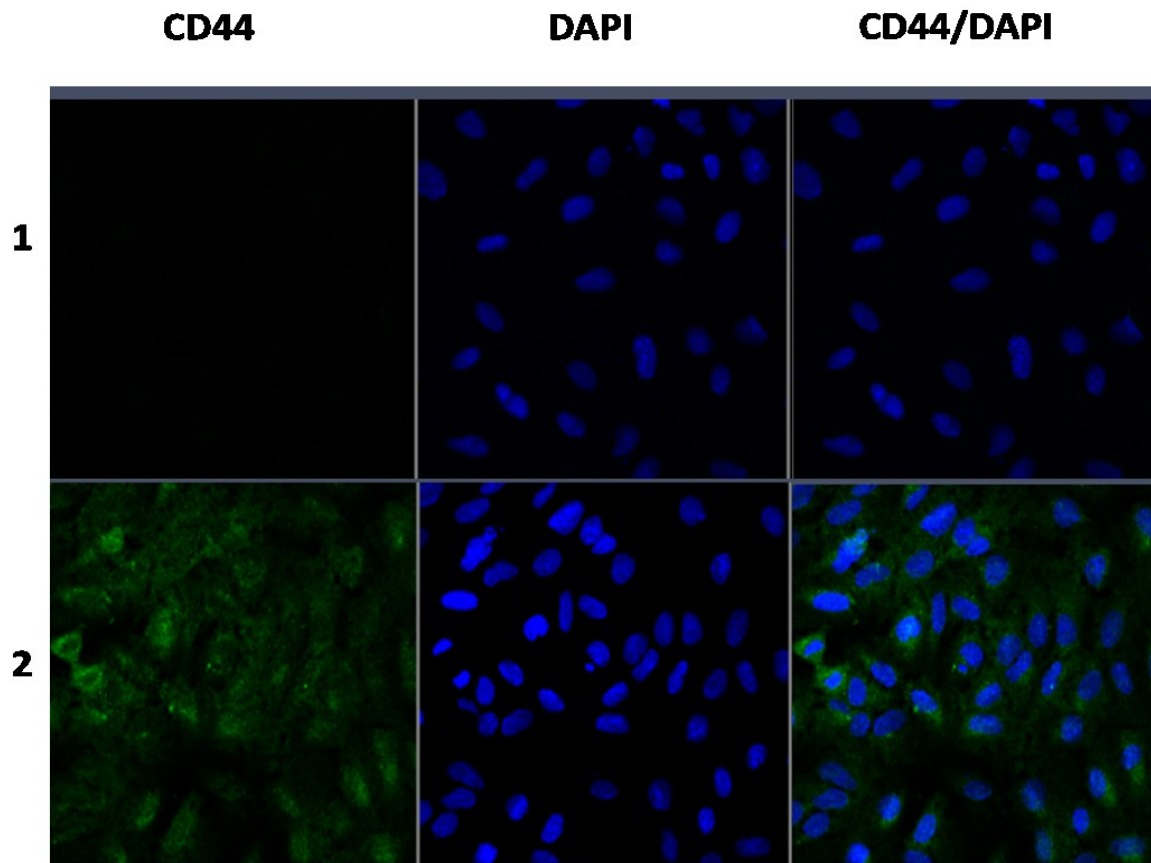
2.3.4 Cytotoxicity

In order to investigate the cellular viability of ARPE-19 cells incubated with HA-lipoplexes, we analyze the cytotoxic response of two different concentrations of siRNA incorporated into the nanoparticles. Untreated ARPE-19 cells were used to normalize the values demonstrated in **Figure 04.** In this experiment, the treatment with 37.6nM of siRNA in HA-lipoplexes did not exhibit cytotoxicity and also promoted a significant increase in metabolic activity of ARPE-19 cells, compared to untreated cells. However, when the double concentration of HA-lipoplex was tested, it significantly reduced the cell viability compared with the control, showing high cytotoxicity effects. As minimal cytotoxicity is important to reduce non-specific effects and cellular mortality, the first concentration tested was selected for the next studies.

Figure 04. Metabolic activity of ARPE-19 cells after incubation with different concentrations of HA-lipoplex, measured by MTT assay and normalized with untreated cells (n=3). Error bars represent the standard deviation (*) p <0.005 compared to the untreated cells (One-way ANOVA and post-test of Bonferroni).
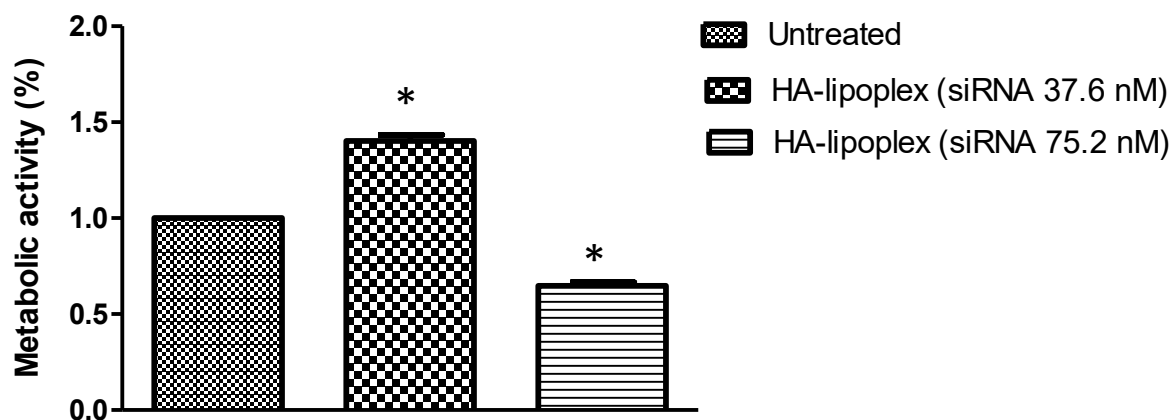
2.3.5 Uptake and transfection of HA-lipoplex

The uptake of lipoplexes prepared with Rhodamine-labelled siRNA was assessed by confocal images. As it can be seen in **Figure 05**, when Rhodamine-labelled siRNA was used to prepare HA-lipoplex, it was possible to observe a cytoplasmic red punctuated fluorescence, demonstrating the internalization of these systems (**Figure 05, A-D**). Indeed, using the confocal orthogonal images, we showed clear evidence of siRNA transfected in ARPE-19 cells (**Figure 05, E**). Also, Lipofectamine® containing Rhodamine-labelled siRNA, used as a reference for positive control, demonstrated the same profile showing a fluorescent sign of siRNA in the cytosol (**Figure 06**). On the other hand, there is no evidence of fluorescence siRNA when the negative control was incorporated into lipoplexes coated by acid hyaluronic **(Figure 06).**

Next, Rhodamine-labelled siRNA was used to compare with naked siRNA, HA-lipoplex and Lipofectamine® siRNA fluorescence in ARPE-19 cells after 48h of incubation (**Figure 07, A**). According to the results, naked siRNA showed the lowest transfection efficiency. Lipofectamine® and HA-lipoplex results indicated that they were able to improve siRNA transfection efficiency, showing the statistical difference to naked siRNA. Finally, comparing Lipofectamine® with HA-lipoplex, our approach showed an efficiency of nucleic acid internalization at about four times higher than the material used as a reference, when both received the same amount of siRNA during preparation. Additionally, it was tested if HA-lipoplex can introduce plasmids and induce the RFP expression in retinal cells. After 48 h of the experiment, HA-lipoplex and Lipofectamine® also showed RFP fluorescence response in ARPE-19 (**Figure 07, B**).

Figure 05. Cellular uptake of HA-lipoplex containing a fluorescent siRNA in ARPE-19 cells. Representative images of serial optical sections collected for three-dimensional reconstruction of: (A) α-tubulin in green; (B) Lamin B1 in purple; (C) and (D) cellular internalization of HA-lipoplexes containing Rhodamine-siRNA; (E) clearly visible Rhodamine-siRNA transfected into ARPE-19 cells showed by orthogonal image (x-z sections at the top and y-z sections at the right of image) obtained in Zeiss LSM 880 confocal microscope.

65

Figure 06. Cellular uptake of negative and positive siRNA controls in ARPE-19 cells. Representative images of serial optical sections collected for three-dimensional reconstruction of: (A) and (E) α-tubulin in green; (B) and (F) Lamin B1 in purple; (C) and (D) cellular internalization of HA-lipoplexes containing siRNA control, with absence of fluorescence; (G) and (H) cellular internalization of Lipofectamine 2000 containing Rhodamine-siRNA. The Zeiss LSM 880 confocal microscope was used to obtain the images.

NEGATIVE CONTROL

POSITIVE CONTROL

Figure 07. (A) Mean fluorescence intensity of Rhodamine-siRNA after 48 h of incubation with ARPE-19 cells (naked siRNA, associated with Lipofectamine® or HA-lipoplex). Transfection results were normalized with cell protein concentrations (n=3). Error bars represent the standard deviation (*) $p < 0.005$ compared to the untreated cells (One-way ANOVA and post-test of Bonferroni). (B) Fluorescence intensity of ARPE-19 cells after incubation with RFP plasmids associated with HA-lipoplex or Lipofectamine®.
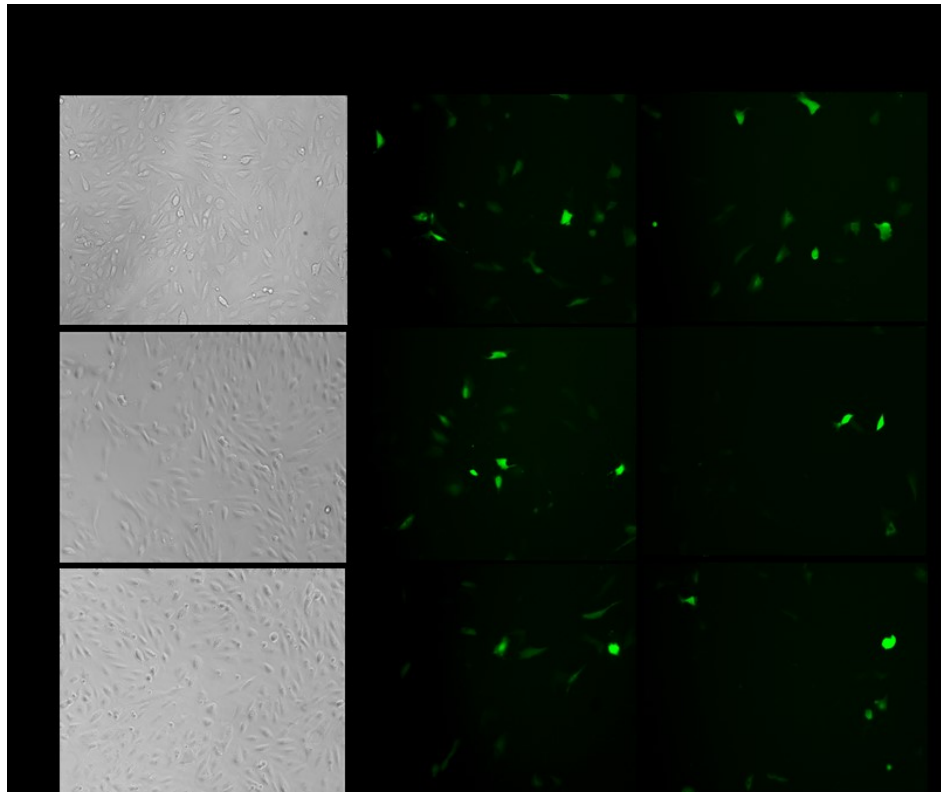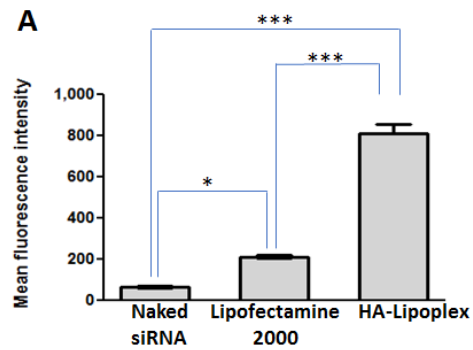
2.4 DISCUSSION

This work aimed to obtain an efficient non-viral vector for the intravitreal delivery of siRNA, with easy preparation and high transfection efficiency. Recently, our research group developed a promising lipoplex system containing sodium alginate to deliver siRNA *in vivo* (ARRUDA et al. 2019). However, for an intravitreal application, it is expected that these systems will not reach the retinal tissues due to their positive superficial charge. Based on this, we planned to functionalize the lipoplex surface with hyaluronic acid. To this purpose, first we evaluated the influence of two different HA molecular weight in the liposome physicochemical properties **(Table 01).** The uncoated cationic lipoplex size was 133.5 ± 1.2 nm and zeta potential + 71.1 ± 3.0 mV. Visible flocculation of these particles was observed when cationic lipoplex was associated with HA solution 0.3 % (w/v) prepared with a low molecular weight of sodium hyaluronate (8-15 kDa). This precipitation probably occurs because the zeta potential of these particles was close to the zone of isoneutrality, when the zeta potential is zero. Similar results were described by Gasperini et al. (2015) when low concentrations of HA 16 kDa (<20 % w/w) was used to study the formation of an electrostatic complex with cationic liposomes. They concluded that when a partial coating of lipoplex with low molecular weight of HA occurs, it leads the system to aggregation. On the other hand, higher concentrations of HA produced a homogeneous coating of the liposomes and decreased the nanoparticle size close to the pure liposome (GASPERINI et al., 2015). In addition, we tested another HA solution containing the same concentration of sodium hyaluronate, but in higher molecular weight HA (160-600 kDa). In this experiment we obtained monodisperse nanoparticle with anionic surface charge, showing the size of 221.8 ± 9.2 nm and zeta potential of - 34.2 ± 1.4 mV. As the overall charge and shape of lipoplexes are related to the structure of the lipid and conditional adjustments, an increase in lipoplex size and zeta potential values in comparison to uncoated one was associated with an electrostatic binding of HA onto the lipoplex surface. Martens and collaborators (2015) also investigated the electrostatic binding of lipoplex using different molecular weights (22 kDa, 137 kDa and 2700 kDa). These authors also obtained a monodisperse nanoparticle with anionic surface charge using an HA solution of 137 kDa

(MARTENS et al., 2015). Regarding the morphology, TEM images showed spherical multilamellar vesicles, with similar size in accordance with DLS studies.

Next, we evaluated if the HA coating could interfere with the siRNA encapsulation in lipoplexes. In the present work, this was evaluated by electrophoresis comparing the band size of siRNA without complexation and the band size of siRNA released from nanoparticles after the treatment with NaCl 1M and Triton-100X, which promote the lipoplexes dissociation (**Figure 02**). Without the treatment addition, there is no evidence of the siRNA band, indicating that uncoated and HA-lipoplex nanoparticles were able to encapsulate the siRNA (**Figure 02,** band 03 and band 05). The band of released siRNA from both nanoparticles after treatment showed an electrophoretic migration comparable and similar to the naked siRNA band migration. Based on this, we can suggest that the HA coating did not affect the siRNA load in nanoparticles. These results are according to Taetz et al. (2009), which showed that liposomes (DOTAP/DOPE) HA recovering did not compromise the binding efficiency of siRNA and increase the system stability, compared with the non-modified liposomes.

Nanoparticle interactions with cellular membranes are an important determinant of its functionality and biological effect. Since the CD44 receptor is a major cell surface receptor for hyaluronic acid (HA) and an important adhesion molecule that mediates cell interactions, we expect that this receptor could mediate the HA-lipoplex internalization (SARAIVA et al., 2017; HUANG and HUANG, 2018). Thus, we investigated CD44 expression on ARPE-19 cells surface by immunofluorescence. The results showed in **Figure 03** confirmed its presence at a high level and showed CD44 clustering. These results are in accordance with a study made by Liu et al. (1997), which also investigated the CD44 expression on retinal cells and observed larger variant forms of CD44. These authors suggested that CD44 expression differs depending on the proliferative status of the cells. In addition, Martens and co-works (2015) studied the participation of the CD44 receptors in the internalization of HA-coated nanoparticles and also confirmed the presence of CD44-expression on ARPE-19 by flow cytometry.

The cellular viability of ARPE-19 cells incubated with HA-lipoplexes was demonstrated in **Figure 04.** In this experiment, we observed that the treatment with 37.6nM of siRNA in HA-lipoplexes was not cytotoxic and also promoted a significant increase in metabolic activity of ARPE-19 cells, compared to untreated cells. This increase in cell viability may be due to one of the numerous HA biological functions, which include the promotion of cell proliferation, migration, and intracellular signaling (HUANG and HUANG, 2018). In sequence, the intracellular uptake of HA-lipoplex in ARPE-19 cells was evaluated using confocal images. Lipofectamine® was used as a positive control and siRNA without fluorescence as the negative control. After overnight incubation of these systems with ARPE-19 cell, in **Figure 05** it is possible to observe Rhodamine-siRNA as red punctuated fluorescence accumulated in retinal cells, delivered by AH-lipoplex and Lipofectamine®. Moreover, using the confocal orthogonal images we showed clear evidence of siRNA transfected in the cytoplasm of ARPE-19 cells (**Figure 05, E**). Therefore, HA-lipoplex could facilitate the intracellular delivery of siRNA into ARPE-19 cells, despite their negative superficial potential. We suggest that the positive uptake of HA-lipoplex might have been thought the interaction between HA of these nanoparticles and the CD44 receptors on ARPE-19 cells, but further studies must be done to confirm it.

Transfection studies can be carried out using liposomes as they can to fuse with the cell membrane and deposit their cargo inside (MA et al, 2007; JANICH et al, 2015). In our study, we compared naked double-stranded siRNA, HA-lipoplex and Lipofectamine® transfection efficiencies of siRNA by fluorimetry. According to the results, we confirmed that naked siRNA showed the lowest transfection efficiency due to its natural properties that difficult their cell internalization and degradation. Lipofectamine® and lipoplex results showed increased values of siRNA fluorescence, indicating an improvement of transfection efficiency with a statistical difference to naked siRNA. Finally, comparing Lipofectamine® with HA-lipoplex, our approach was approximately four times more effective than Lipofectamine® to the transfect the same amount of siRNA to ARPE-19 cells. These results highlight the HA-lipoplex advantages to complex and transfect siRNA to ARPE-19 cells. Moreover, the gene expression by the incorporation of pAd-

RFP reinforced the good properties of our system as a non-viral vector of nucleic acids. These results are in accordance with Wojcicki and collaborators (2012) that developed cationic liposomes targeting the CD44 receptor with an incorporation of a conjugate between high molecular weight HA and the lipid DOPE (HA-DOPE). According to the authors, lipoplexes at a lipid:DNA ratio of 2 containing 10% (w/w) of HA improved the transfection efficiency comparing to the uncoated lipoplex (WOJCICKI et al., 2012).

2.5 CONCLUSION

In conclusion, this study indicated that we could successfully functionalize cationic lipoplex with hyaluronic acid. These nanoparticles were able to protect and deliver siRNA into ARPE-19 cells, showing low cytotoxicity and high efficiency in transfection studies. Based on this, HA-lipoplex is an attractive nanoparticle to deliver therapeutic siRNA to retinal cells and a promising system for *in vivo* studies.

3. CHAPTER 03: Experimental work

Lipoplex coated with hyaluronic acid for safe and efficient intravitreal delivery of siRNA to the retina

3.1 INTRODUCTION

Drug delivery plays an important role in current retinal therapeutics and the development of new medications. Currently, despite many blinding disorders that affect retina have a well-known genetic background, there is no treatment able to recover the vision of patients after they lose retinal cells by a degenerative process (PASCOLINI and MARIOTTI, 2012; HUANG, CHEN and RUPENTHAL, 2018). Since the possibility of control gene expression via small interfering RNA (siRNA) has become a reality in pre-clinical and clinical trials, this new technology has been widely studied in order to promote treatment and even cure of retinal genetic dysfunctions (THAKUR et al. 2012; ZULLIGER, CONLEY, and NAASH, 2015; SARAIVA et al., 2017; SHEN et al., 2018).

The eye appears particularly attractive for RNAi studies. Indeed, it is easily accessible, relatively immune-privileged and small, which makes it possible to obtain a therapeutic effect with low amounts of the drug (WANG, RAJALA and RAJALA, 2015; PETIT, KHANNA, and PUNZO, 2016). In addition, the monogenic nature of retinal diseases and the recent knowledge of their molecular pathogenesis contribute for the ocular genetic therapy research, showing more than 260 genes and loci related with retinal disease mapped in genetic basis (http://www.sph.uth.tmc.edu/RetNet/) (ADIJANTO and NAASH, 2015; OLIVEIRA, ROSA DA COSTA and SILVA, 2017).

Besides the several ocular properties that impulse its application as a target for therapeutic nucleic acids, the effectiveness of RNAi significantly depends on the siRNA vector ability to overcome natural barriers of the eye and reach the retinal tissues. Intravitreal administration is an important route to increase the bioavailability of nucleic acids in the posterior segment of the eye. In contrast to subretinal injection, which promotes a local retinal detachment, intravitreal injection may be most clinically acceptable as an ocular route because it is simpler, less invasive and allows an introduction of larger molecules and higher doses of drug (SOLINÍS et al., 2015; OLIVEIRA, ROSA DA COSTA and SILVA, 2017). Even though intravitreal injections have been related to increased ocular pressure and a small risk of endophthalmitis,

these possible post-injection complications can be easily managed and cannot be compared to the risks of other intraocular administration routes (ISSA and MACLAREN, 2011; ENGLANDER et al., 2013; MARTENS et al., 2017).

Viral and non-viral vectors can be employed to deliver nucleic acids to the retina. However, relevant concerns related to the persistence of viral vectors, risk of oncogenicity and immunogenicity have supported the interest to invest in non-viral carries (YU-WAI-MAN et al., 2016; XIA, TIAN and CHEN, 2016). Liposomes have emerged as a leading non-viral vector for the intraocular delivery of siRNA. These vehicles can protect nucleic acids from degradation by endogenous nucleases and for tissue targeting. Moreover, they are biocompatible, biodegradable, show almost no toxicity and low antigenicity in several studies. Among various liposomes described in the literature, the association between cationic liposomes and siRNA called (lipoplex) are the most investigated nanoparticles for gene silencing studies. However, this positive charge of cationic lipoplex can be detrimental for its mobility and induce a severe aggregation in contact with the vitreous humor. Also, a thin layer of vitreous on top of retinal cells almost completely blocks the gene expression of cationic lipoplexes (PITKÄNEN et al., 2003; PEETERS et al., 2007; BOCHOT and FATTAL, 2012).

Recently, Martens et al. (2017) developed an *ex vivo* model for testing nanoparticle mobility in the vitreous humor and suggested that lipoplex coated with HA are promising drug delivery for this goal, but these authors did not evaluate *in vivo*. Therefore, the aim of the present study was to investigate the safety and efficiency of lipoplex strategically coated with HA to deliver siRNA to retinal tissues after intravitreal injections.

3.2. MATERIALS AND METHODS

3.2.1 Animals

Adult male Wistar rats with a body weight of 180-200 g were used. The rats were housed in a 12-hour light-dark cycle. All experiments were conducted in accordance with the guidelines of the Association for Research in Vision and Ophthalmology (ARVO). The ethics protocol was approved by the commission on ethics on the use of animals of the Federal University of Minas Gerais (Comissão de Ética no Uso de Animais, CEUA-UFMG), under protocol 31/2019. All the animals received food and water *ad libitum*.

3.2.2 siRNAs

Rhodamine-labeled siRNA and a non-silencing siRNA (50 UUC UCC GAA CGU GUC ACG UdTdT 30) used as negative control were purchased from Eurogentec.

3.2.3 Liposomes and lipoplexes

Cationic liposomes were prepared as reported previously by our research group (RHINN et al., 2009; HAMOUDI et al., 2015), composed by DMAPAP cationic lipid (RPR 209120 2-{3-[Bis-(3-amino-propyl)-amino]-propylamino}-N-ditetradecyl carbamoyl methyl-acetamide) and DOPE (1,2-dioleoyl-sn-glycero-3-phosphoethanolamine) obtained from Avanti Polar Lipids. First, to obtain the liposomes, a chloroformic solution of an equimolar mixture of DMAPAP and DOPE is prepared. Then, the organic solvent was evaporated under vacuum to form a thin lipid film, using a rotary vacuum evaporator at 20 °C. After this process, this lipid film is rehydrated to produce large multilamellar vesicles and sonicated (115 V, 80 W, 50–60 Hz) with a G112SP1G model sonicator (Laboratory Supplies Co. Hicksville, N.Y.) to obtain a homogeneous suspension of liposomes.

Lipoplexes were prepared by mixing 1.5 µg of siRNA (control or Rhodamine-labelled) and sodium alginate solution (Sigma-Aldrich) at ratio 1:1 (w/w) in 150 µL of NaCl 150 mM, with an equal volume of the cationic liposome suspension prepared also in 150 mM NaCl. Lipoplexes were allowed to form for 30 min at room temperature before use. The

charge ratio of cationic lipoplexes was R+/- =8, calculated using the molar ratio of positive charges (positive charges per molecule of DMAPAP) to the molar ratio of negative charges (from siRNA and anionic polymer molecules, respectively siRNA 3.03 and AA 5.05 nmoles of negative charges/mg).

For coating lipoplex with hyaluronic acid (Bio-sodium hyaluronate powder, 160-600 kD), the cationic lipoplexes were rapidly mixed by vortexing with an equal volume of hyaluronic acid solution 0.3 % (w/v).

3.2.4 Intravitreal injections of lipoplex

The rats were anesthetized with an intraperitoneal injection of ketamine 80 mg/kg and xylazine 8 mg/kg before the intravitreal injection. A drop of 0.4% oxybuprocaine hydrochloride was also applied in each rat eye to perform local anesthesia of the cornea. Five microliters of different lipoplex (cationic and coated with HA) or physiologic saline solution were injected into the posterior side of the globe by syringes BD ultra-FineTM 6mm x 31G needles (BD).

3.2.5 Electroretinogram

ERG was performed using an Espion (Diagnosys LLC, Cambridge, UK). The cationic lipoplex and lipoplex-HA were prepared as previously described in NaCl (150 mM, pH 7.4) for the intravitreal administration. Electrophysiological measurements were performed after the intravitreal injections, at 7 and 14 days of this procedure in two groups of rats: one group that received five microliters of cationic lipoplex (n=4) in the left eyes and the other group that received lipoplex-HA. The contralateral eyes in both groups served as control and were injected with five microliters of sterile physiological saline.

Before the ERG exams, the rats were kept in total darkness for 12h. After this period, animals were anesthetized by intraperitoneal injections of ketamine 80 mg/kg and xylazine 8 mg/kg before the exam to reduce electrical or movement interference. Pupils were dilated with 0,5 % tropicamide (Midriacyl®, São Paulo, Brazil). In addition, a drop

of 0.4% oxybuprocaine hydrochloride was also applied to perform local anesthesia of the cornea. The contact lens electrodes (Rodent Contact Lens, Ocuscience) were carefully adapted over the cornea of the animal and the reference and groud electrodes (Stainless Steel Subdermal Needle Electrode, Ocuscience) were placed between the eyes and on the tail, respectively. During the experiment, animal preparation and ERG conditions were performed on low red light intensity.

The ERG protocol consisted of 3 steps: rod peak response, scotopic maximum response, and a photopic response. Rod peak response and scotopic maximal response ERGs were elicited using stimulus intensities between 0,00003 cd.s/m^2 and 3 cd-s/m², respectively, on a dark background. After light adaptation for 10 minutes, photopic ERGs were elicited using 3 cd-s/m² on a white background of 30 cd/m², from 15 Hz until 45 Hz. For each recording, 15 separate responses were averaged in the ERG recording system, including the amplitude and latency of each waveform. All procedures were performed in accordance with the standards recommended by the International Society of Clinical Electrophysiology of Sight (ISCEV). Statistical analysis in ERG measurements was conducted using ANOVA and Tukey post-test and data were analyzed as the mean ± standard deviation (SD).

3.2.6 Clinical evaluation

The clinical ophthalmic evaluation of all animals was performed by a veterinary ophthalmologist. The indirect ophthalmoscopy (Omega 500 Binocular Indirect Ophthalmoscopy, Heine optotechnik, Germany) was done before the intravitreal injections and after at the predetermined intervals of 7 and 14 days. Also, the fundus examination was done using 90 D lens (Wlch Allyn, USA). The intraocular pressure (IOP) of both eyes of each rat was assessed by a portable tonometer Tonopen XL (Reichert New York, USA). Before IOP measurements, each eye was anesthetized in the cornea with a drop of 0.5% proxymetacaine hydrochloride (Anestalcon; Alcon, São Paulo, Brazil). To reduce variations, IOP was assessed between 12:00 pm and 13:00

pm of each day or week. Three IOP readings were obtained from each eye and these results were expressed as the group mean IOP ± SD.

3.2.7 Histological evaluation

After the last ERG recording on day 14, the rats were euthanized (n=8) and their eyes were enucleated and immediately fixed in Karnovsky's Fixative (cacodylate buffer 0,1 M, pH 7.4). Then, these eyes were rinsed in cacodylate buffer (cacodylate buffer 0,1 M, pH 7.4) and dehydrated in an ascending series of alcohols to be embedded in paraffin. Tissues sections of 4-µm were cut and stained with hematoxylin and eosin for light microscopy investigation (Zeiss®, Model Axio Imager M2).

3.2.8 Retinal distribution of lipoplex

The cationic lipoplex and lipoplex-HA were prepared as previously described in NaCl (150 mM, pH 7.4), For the biodistribution study, the animals were divided into two groups, according to the lipoplex formulations. In the first group (n=4), five microliters of cationic lipoplex containing Rhodamine-labelled siRNA were administered thought intravitreal injections in each left eye of these rats. Similarly, the second group of animals (=4) received by intravitreal injections five microliters of lipoplex-HA containing Rhodamine-labelled siRNA in each left eye of these rats. The contralateral eyes in both groups served as control and were injected with five microliters of lipoplex containing control siRNA without fluorescence.

Three hours after intravitreal injections, the rats of this study were euthanized. Their eyes were enucleated and fixed immediately with 4 % paraformaldehyde solution (PFA). On the next day, these samples were washed with PBS and incubated with sucrose solution in PBS at room temperature before the inclusion in OCT compound. Then, the eyes were frozen and immediately stored at −80 °C until sectioning. The 10 µm cryo-sections were prepared by using a cryostat (LeicaCM3050S). The Zeiss LSM 5 Live (Carl Zeiss) confocal microscope was used to obtain the images of retinal tissues.

3.3 RESULTS

3.3.1 Electroretinogram

ERG was performed 7 and 14 days after the intravitreal injections. During the scotopic condition, dark-adapted animals were exposed to increasing luminance to assess the a-wave and b-waves amplitudes, and implicit times. The ERG responses were expressed in **Figure 01**, considering the treatment test eyes and contralateral eyes in 0,01 cd.s/m^2 (rod response) and 3 cd.s/m^2 (maximal or standard combined rod-cone). In sequence, the animals were also examined in light-adapted conditions by single-flash cone response and flicker ERG in 3 cd.s/m^2. Dark-adapted a, and b-wave amplitudes were not significantly altered in eyes that received cationic lipoplex, HA-lipoplex or saline during the 7 and 14 days of this experiment (p>0,05, p=0,5439). Also, similar results were found in light-adapted animals and no statistically significant differences were found between the rat eyes that was received saline with the others that received lipoplex (p>0,05, p=0,5927). The mean ± SD of Vmax and k parameters of the Naka-Rushton function and their relation with the increasing luminance for all groups are exhibit in **Figure 02**.

Figure 01 - Graphical ERG measurments expressed of darkness-adapted a and b-waves in the experimental eyes with a stimulus of 0.01 cd.s/m² and 3,0 cd.s/m² (A,B and C). Representative ERG responses according to luminance and implicit time in darkness-adapted (D,E) and light adapted conditions (F,G).
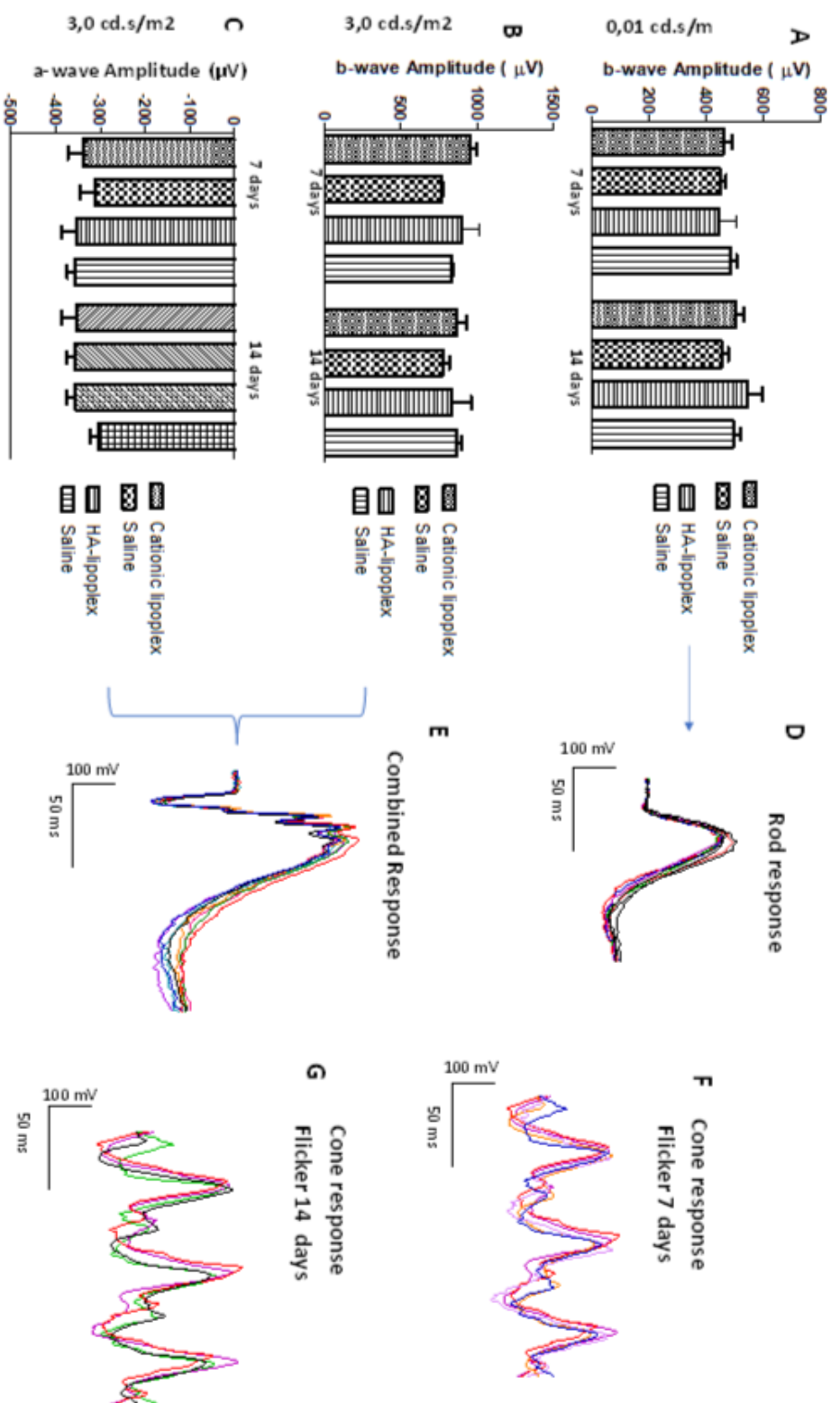
Figure 02- Representatives ERG responses considering the Naka-Rushton function (A), Vmax (B) and k parameters (C) of the relation between dark-adapted b-wave amplitude and luminance. ERG was performed 7 and 14 days after the intravitreal injections.
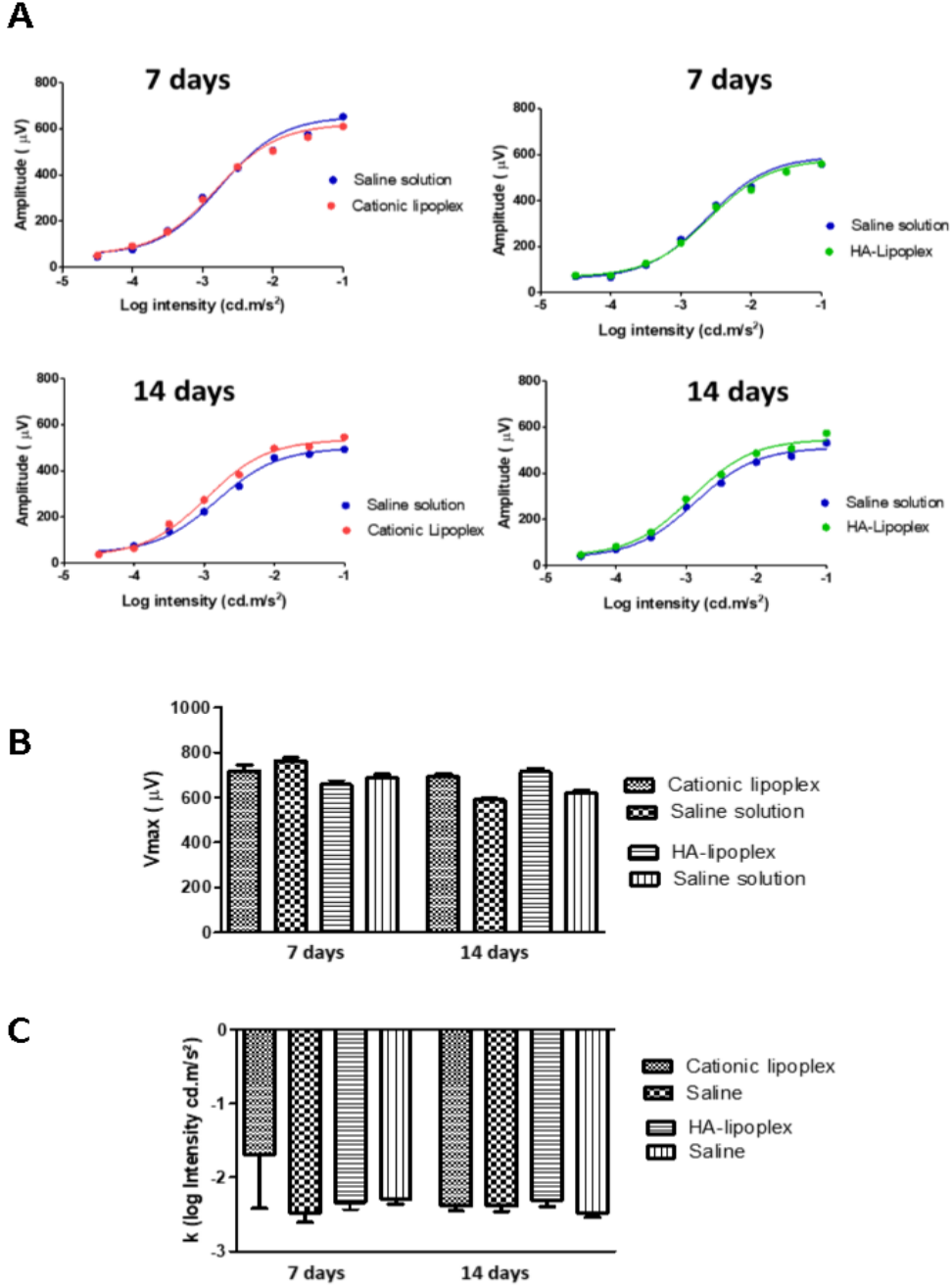
3.3.2 Clinical evaluation

No ocular damage such as corneal edema, hyperemia or conjunctival secretion, hemorrhaging, vitreous opacity and retinal detachment was observed during the clinical evaluation. However, one animal that received saline injection developed cataract one day after the intravitreal injection. As the cataract was related to the intravitreal injection procedure and not to the lipoplex formulations, this animal was excluded from this study. (**Figure 03**). In each animal, ocular fundus examination and images were registered as showed in **Figure 04**. Regarding the IOP measurements, despite the IOP variations during the experiment, these eyes showed the main values in the normal range of rat IOPs (16,5 ± 5,4 for saline and 14,5 ± 3,4 for H-lipoplex) (**Figure 05**).

Figure 03 -Ocular clinical evaluation. Rat eye before the intravitreal injection (A), rat eye immediately after intravitreal injection (B), rat eye with cataract (C).
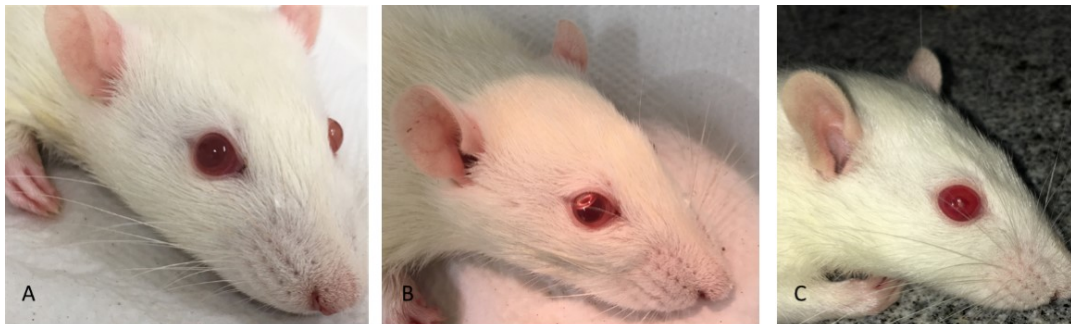
Figure 04 -Representative images of ocular fundus examination after intravitreal injection of physiological saline (A), cationic lipoplex (B) and HA-lipoplex.
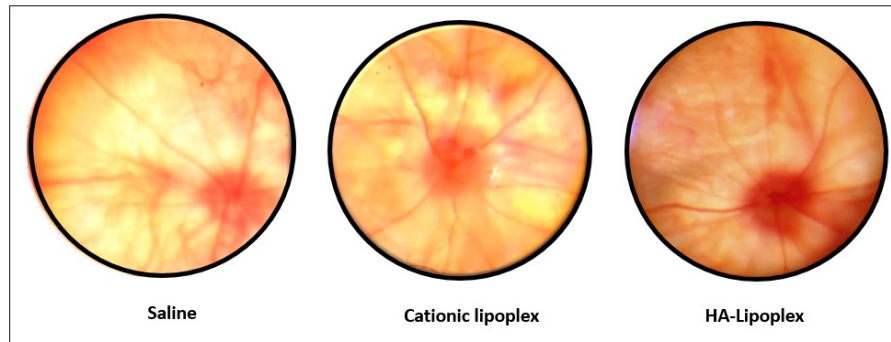
Figure 05- Rat eyes intraocular pressure at different times of the study (Mean ± SD).
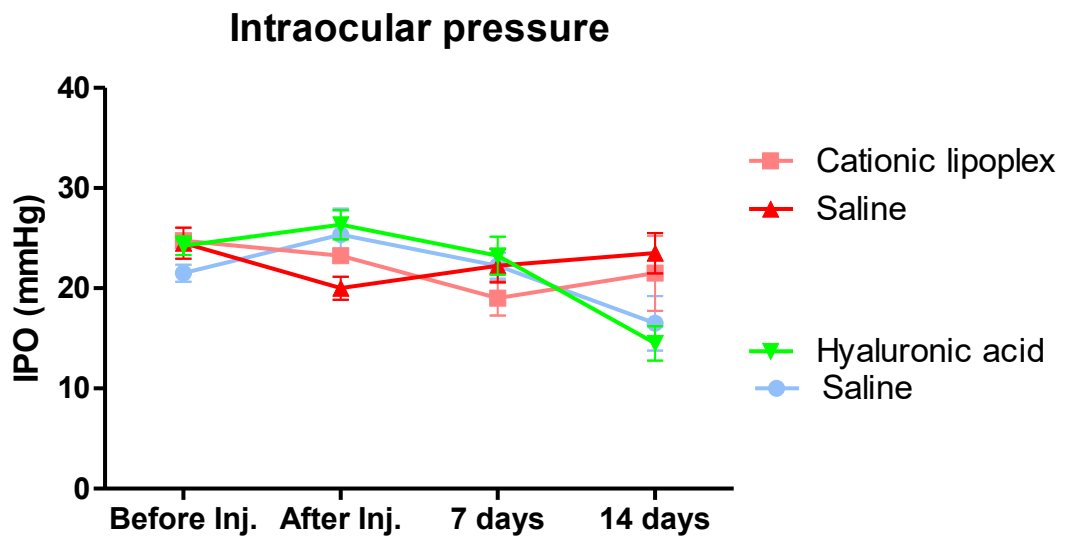
3.3.3 Histology

Histological examination of rat retinas with light microscopy did not show any abnormality or changes in retinal layers morphology, as showed in **Figure 06**.

Figure 06 - Example of retinal sections from one rat eye submitted to intravitreal injection of physiological saline (A), cationic lipoplex (B) and HA-lipoplex, after 14 days of injections. GCL, ganglion cell layer; INL, inner nuclear layer; ONL, outer nuclear layer.
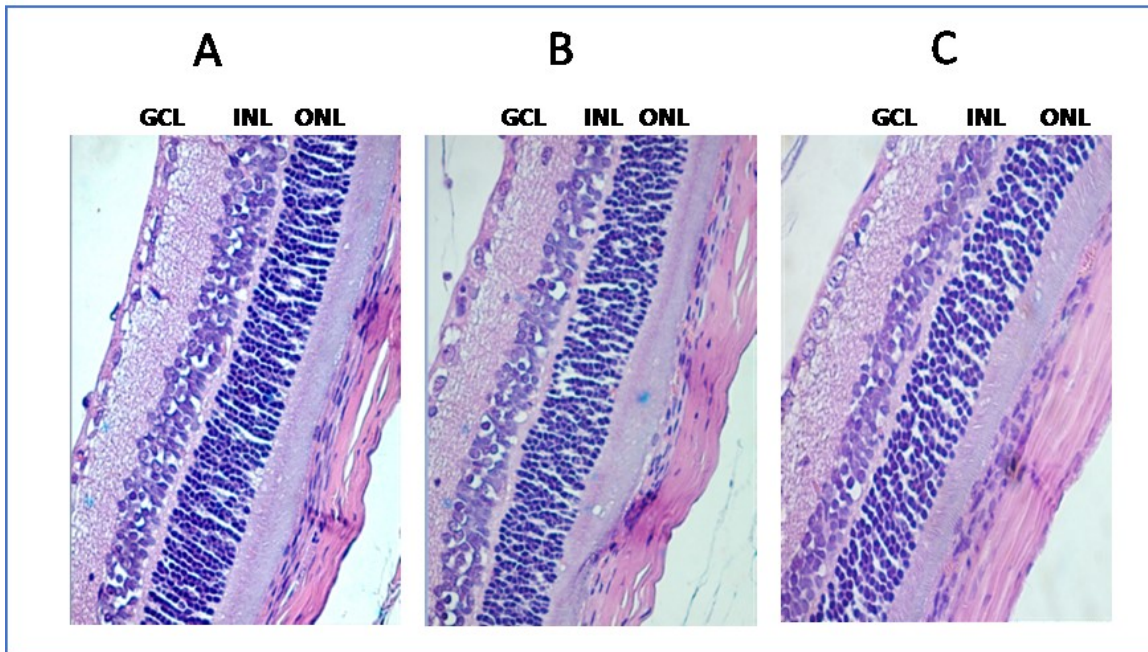
3.3.4 Retinal distribution of lipoplex

The distribution of both lipoplex in the retina 3 hours after intravitreal injections is indicated in confocal images (**Figure 07)** by the fluorescence intensity of Rhodamine-siRNA in different retinal layers. The siRNA delivered by cationic lipoplex was accumulated in the ganglion cell layer but was not able to reach deeper retinal structures. In contrast, the HA-lipoplex could overcome the inner limiting membrane and the fluorescent siRNA was detected in the inner and outer nuclear layers, and RPE. No fluorescence could be detected when the control siRNA was used in contralateral eyes.

Figure 07 Representative fluorescence images of siRNA retinal distribution obtained from samples 3 h after intravitreal injections. The rats received intravitreal injections of lipoplex containing non-fluorescent siRNA in the left eyes (A and B), cationic lipoplex containing rhodamine-labelled siRNA (C and D) and lipoplex containing rhodamine-labelled siRNA (E and F). The images were obtained using Zeiss LSM 5 Live (Carl Zeiss) confocal microscope. GCL, ganglion cell layer; INL, inner nuclear layer; ONL, outer nuclear layer; RPE, retinal pigment epithelium.
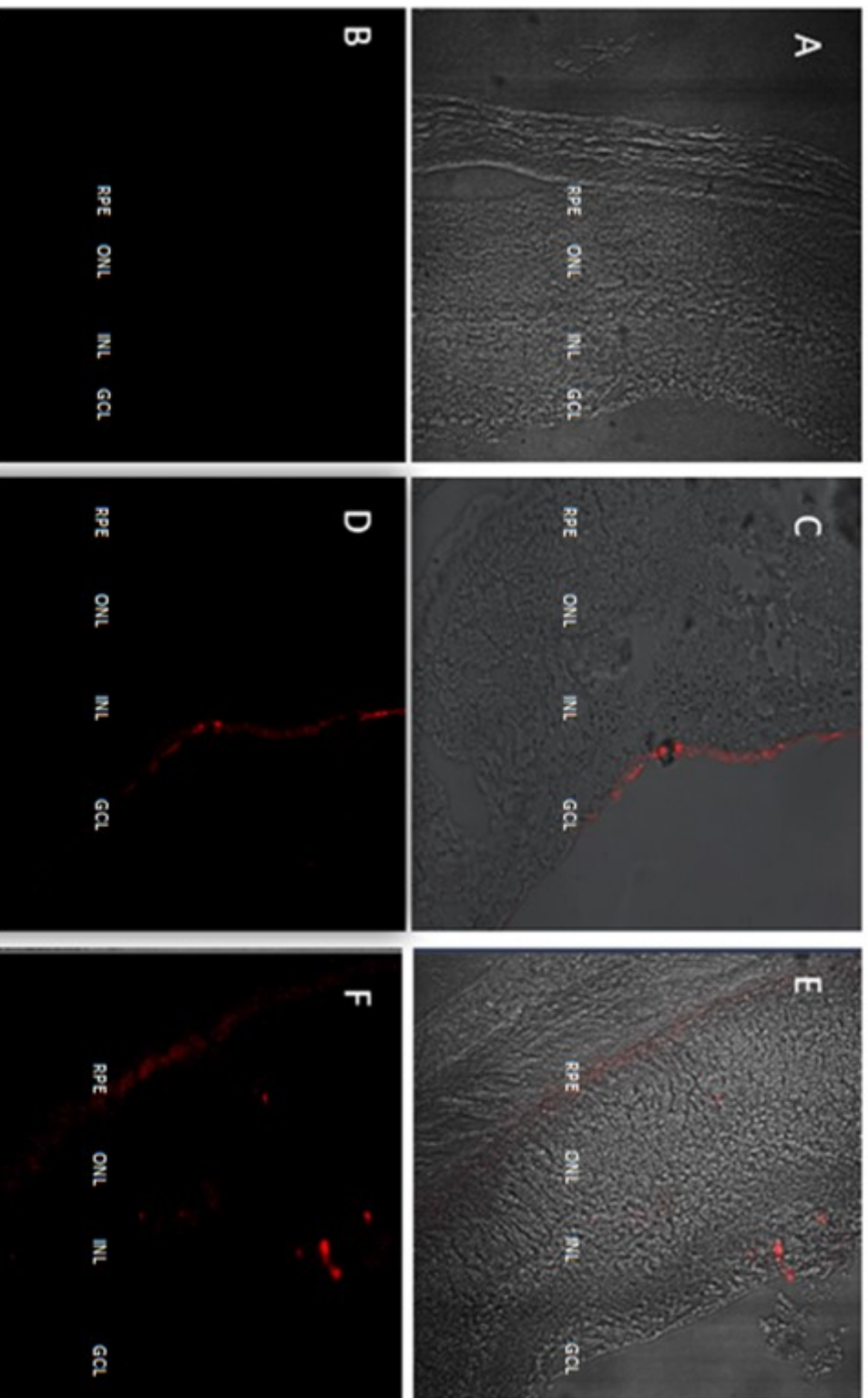
3.4 Discussion

The RNAi therapy success relies on the siRNA delivery vector suitability to overcome intraocular barriers and reach retinal tissues. Until now, questions have been raised about the feasibility of cationic lipoplex electrostatic coated with HA to deliver siRNA *in vivo*. Thus, in this study, the uncoated lipoplex was compared to the same system functionalized with HA in terms of siRNA delivery efficiency and safety after intravitreal injection. The retinal distribution assay results demonstrated that both lipoplexes could transport the siRNA thought intravitreal cavity and also facilitate this nucleic acid internalization in retinal tissues a few hours after intravitreal injections. Despite the cationic charges, uncoated lipoplex could overcome the vitreous barrier and reach the ganglion cell layer. However, they could not penetrate into deeper retinal layers. On the other hand, the fluorescent siRNA delivered by HA-lipoplex could be seen in both outer and inner retinal layers and accumulated in the RPE.

These results are according to Koo et al. (2012), which studied the correlation between the surface and the distribution of different types of nanoparticles in the vitreous and retina. In this study, four different polymers such as polyethyleneimine (PEI), glycol chitosan (GC), hyaluronic acid (HA), and human serum albumin (HSA) were used as hydrophilic shell polymers of nanoparticles labeled with fluorescent dyes. These authors demonstrated that while HA and HAS nanoparticles showed superior penetrating ability across the whole retina, strongly cationic charged nanoparticles prepared with PEI was found stuck to the vitreous, and cationic systems made with GC did penetrate through the physical pores of inner limiting membrane into the retinal structure. One important advantage of lipoplex-HA compared to HA or HAS polymeric nanoparticles for acid nucleic delivering is the spontaneous complexation with siRNA, property that anionic polymeric systems do not have. Also, to explain how HA and HSA overcame the physical barriers of the inner limiting membrane, the biodistribution of these nanoparticles were investigated by TEM and immunohistochemistry. They found that the interaction with Müller cells was an important mechanism of these anionic nanoparticle's internalization into the deeper retinal structures. Therefore, we suggest that the lipoplex-

HA may be able to across the retina and reach RPE by the same mechanism related to Müller cells, but further studies must be done to confirm this.

Not only the surface modification of lipoplex-HA but also the route of administration was essential to reach this result. Previous studies showed that the bioavailability of nucleic acids in the posterior segment of the eye after topical instillation is very poor, especially because of their size (BLOQUEL et al., 2006; SOLINÍS et al., 2015). Systemic administration shows similar results and only 1–2% of the therapeutic molecules administered can reach the vitreous cavity, due to the existence of the blood-retinal barrier (OLIVEIRA, ROSA DA COSTA and SILVA, 2017; DIAS et al. 2018). In addition, retinal delivery systems could be accomplished using other routes such as periocular (sub-conjunctival, sub-Tenon's, peribulbar and retrobulbar injections) and suprachoroidal. However, these approaches may not result in adequate drug concentrations in the retina with currently available technologies (DEL AMO et al., 2017). As intravitreal injection can be used for a direct insertion of nucleic acids in the posterior segment of the eye, this administration provided a good distribution and an extensive uptake of this siRNA by retinal tissues.

Next, in order to investigate the safety of lipoplex after intravitreal injections in retina, this study combined visual electrophysiological functional exams, clinical evaluation and histologic assays. To assess the visual pathway of retina, ERG exams were performed 7 and 14 days after intravitreal injection of both lipoplexes. Considering the a and b-waves amplitudes in both scotopic or photopic conditions of ERG, statistical analyses showed no significant changes in their values during the experiment. Contributing to these findings, the Naka-Rushton hyperbolic function results showed very similar b-wave amplitude responses between treatment and contralateral eyes, when they were exposed to a progressive increasing in light stimulus **(Figure 2).** Based on these study findings, intravitreal administration of cationic and HA-lipoplex may not interfere on rod and cones functionality.

These results were in accordance with clinical evaluation of rat's retina, which showed no apparent toxicities of lipoplex *in vivo.* In order to evaluate the internal ocular health, the fundus examination was done and no damage changes were observed before and after intravitreal injections (**Figure 04).** Regarding the IOP measurements, the rat group that received the HA-lipoplex and saline in the contralateral eye exhibit an expressive IOP reduction in both eyes at 14 days after the intravitreal injections, compared to the other group (**Figure 05**). According to Mermoud et al. (1994), which established the normal range of IOPs in Lewis rats using the Tono-Pen tonometer, with a 90% confidence interval, the values were 7.28 mm Hg for the lower limit and 26.98 mm Hg for the higher limit. Based on this, despite the IOP variations found in this animal group, these eyes showed the main values in the normal range of rat IOPs (16,5 ± 5,4 for saline and 14,5 ± 3,4 for H-lipoplex). In addition, these authors reported that false-IOP readings could occur after touching the eyelid or lacrimal meniscus, and because of the anesthesia. Since the contralateral eyes showed similar results at the same time of the experiment, the lower intraocular pressure may not be related to the toxic effect of lipoplex.

In addition, the histologic results didn't show significant changes between the eyes that received lipoplex formulations and saline. These findings agree with other histological studies of liposomes after intravitreal injection. In 2002, Bochot et al. investigated the efficacy of liposomes for delivering phosphodiester oligonucleotides intravitreally into rabbits' eye. According to their histologic results, no toxicity was observed, except a localized inflammation in the vitreous on the day following injection, which was linked to the injection itself. Later, Lajavardi et al. (2007) investigated the efficacy of Vasoactive Intestinal Peptide (VIP) encapsulated in liposomes during endotoxin-induced uveitis in Lewis rats. According to these authors, PEGylated liposomes do not cause ocular inflammation 24 h following the intravitreal injections in rats, even at high concentrations (up to 116 mM lipid, corresponding to 1.16 µmol per eye). Also, the clinical evaluation of the rat eyes using the slit lamp biomicroscope 14 days after the injection of 50 mM of this formulation did not evidence any intraocular damaging effect. Finally, according to all the results, cationic lipoplex and HA-lipoplex were considered safe for intravitreal

administrations. Further studies must be done to evaluate the effects of more than one injection at the same eye and different doses of formulations.

.

3.5 CONCLUSION

Our findings in this study demonstrate the relevance of the HA-lipoplex that was developed. The increased internalization of siRNA into retinal tissues confirmed the expectative that these systems could be a valuable system to transport nucleic acids to target cells in the retina. At the same time, the intravitreal injections of lipoplex did not induce apparent toxic effects on the function and morphology of the rat retina.

GENERAL CONCLUSION

Lipoplexes are promising siRNA delivery systems that have been studied for gene expression inhibition. Accurate knowledge of their structure is essential to evaluate the best strategies to improve the in vitro and in vivo efficiency of these nanocarriers. Here, we developed and investigated a novel HA-lipoplexes for the delivering of siRNA into rat retina. *In vitro*, these nanoparticles had already shown good properties as non-viral vectors. Then, the next assays demonstrated for the first time that an easy coating of lipoplex by electrostatic interactions leads to a significant improvement on siRNA delivering in retinal layers, compared to the cationic lipoplex. Moreover, the results suggested that they are safe to the purpose. Therefore, these results open new possibilities for the treatment of many ocular diseases using non-viral vectors, as one of the major limitations of siRNA therapies relies on its delivering.

PERSPECTIVES

The perspectives of this project are:

- The improvement of lipoplex characterization by Small Angle X-ray Spectroscopy (SAXS) analyses;

- Fundamental understanding of the transport and release mechanisms of siRNA from the lipoplex in the posterior segment of the eye.

- The evaluation of lipoplex neuroprotection potential in a retinal light damage model induced by Light Emitting Diodes (LED) exposition in Wistar rats. The gene silencing efficiency will be tested using specific siRNA to prepare lipoplex aiming to promote the retinal cells survival or recovery after excessive exposure to the LED light.

REFERENCES

ADIJANTO, J.; NAASH, M. I. Nanoparticle-based Technologies for Retinal Gene Therapy. **European Journal of Pharmaceutics and Biopharmaceutics**, v. 95, p. 353-367, 2015.

AKBARZADEH, A.; REZAEI-SADABADY, R.; DAVARAN, S.; WOO-JOO, S.; ZARGHAMI, N.; HANIFEHPOUR, Y.; SAMIEI, M.; KOUHI, M.; NEJATI-KOSHKI, K. Liposome: classification, preparation, and applications. **Nanoscale Research Letters**, v.8, p.1-9, 2013.

ALLEN, M.; CULLIS, P. R. Liposomal drug delivery systems: From concept to clinical applications. **Advanced Drug Delivery Reviews**, v. 65, n. 1, p. 36-48, 2013.

ARPICCO, S.; LERDA, C.; DALLA POZZA, E.; COSTANZO, C.; TSAPIS, N.; STELLA, B.; PALMIERI, M. Hyaluronic acid-coated liposomes for active targeting of gemcitabine. **European Journal of Pharmaceutics and Biopharmaceutics**, v. 3, n. 85, p. 373-380, 2013.

ARRUDA, D.C.; GONZALEZ, I.J.; FINET, S.; CORDOVA, L.; TRICHET, V.; ANDRADE, G. F.; HOFFMANN, C.; BIGEY, P.; MACEDO, W.A.A.; CUNHA JR, A. S.; SOUZA, A.M.; ESCRIOU, V. Modifying internal organization and surface morphology of siRNA lipoplexes by sodium alginate addition for efficient siRNA delivery. **Journal of Colloid and Interface Science**, n. 540, p. 342-353, 2019.

BANGHAM, A.D.; STANDISH, M.M.; WATKINS, J.C. Diffusion of univalent ions across the lamellae of swollen phospholipids. **Journal of molecular biology**, v. 13, p- 238-252,1965.

BAREFORD, L.M.; SWAAN, P.W. Endocytic mechanisms for targeted drug delivery. **Advanced Drug Delivery Reviews**, v. 59, n. 8, p 748-758, 2007.

BOCHOT, A.; FATTAL, E.; BOUTET, V.; DEVERRE, J.R.; JEANNY, J.C.; CHACUN, H.; COUVREUR, P. Intravitreal delivery of oligonucleotides by sterically stabilized liposomes. **Investigative Ophthalmology & Visual Science**, v. 43, p. 253–259, 2002.

BOCHOT, A.; FATTAL, E. Liposomes for intravitreal drug delivery: A state of the art. Journal of Controlled Release, v. 161, p. 628–634, 2012.

BLOQUEL, C.; BOURGES, J.; TOUCHARD, E.; BERDUGO, M.; BENEZRA, D.; BEHAR-COHEN, F. Non-viral ocular gene therapy: Potential ocular therapeutic avenues. **Advanced Drug Delivery Reviews**, v. 11, n. 58, p. 1224-1242, 2006.

BOZZUTO, G.; MOLINARI, A. Liposomes as nanomedical devices. **International Journal Of Nanomedicine,** p.975-999, 2015.

BRANDLI A, STONE J. Using the Electroretinogram to Assess Function in the Rodent Retina and the Protective Effects of Remote Limb Ischemic Preconditioning. **Journal of Visualized Experiments,** v. 100, p.1-8, 2015.

CAMERON, M. A.; BARNARD, A. R.; LUCAS, R.J.The electroretinogram as a method for studying circadian rhythms in the mammalian retina. **Journal of Genetics**, v. 87, p. 459-66, 2008.

CROOKE, A.; MEDIERO, A.; GUZMAN-ARANGUEZ, A.; PINTOR, J. Silencing of P2Y2 receptor delays Ap4A-corneal re-epithelialization process. **Molecular Vision**, n. 15, p. 1169–1178, 2009.

DALKARA, D.; SAHEL, J. Gene therapy for inherited retinal degenerations. **Comptes Rendus Biologies,** v. 3, n. 337, p. 185-192, 2014.

DEL AMO, E. M.; RIMPELÄ, A.; HEIKKINEN, E.; KARI, O. K.; RAMSAY, E.; LAJUNEN, T.; URTTI, A. Pharmacokinetic aspects of retinal drug delivery. **Progress in Retinal and Eye Research**, n. 57, p. 134-185, 2017.

DELMONTE, D. W.; KIM, T. Anatomy and physiology of the cornea. **J Cataract Refract Surg,** n. 37, p. 588-598, 2011.

DELPLACE, V.; PAYNE, S.; SHOICHET, M. Delivery strategies for treatment of age-related ocular diseases: From a biological understanding to biomaterial solutions. **Journal of Controlled Release**, n. 219, p. 652-668, 2015.

DIAS, M.F.; JOO, K.; KEMP, J.A.; FIALHO, S. L.; CUNHA JR, A. S.; WOO, S.J.; KWON, Y. J. Molecular genetics and emerging therapies for retinitis pigmentosa: Basic research and clinical perspectives**. Progress in Retinal and Eye Research**, n. 63, p. 107-131, 2018.

DICARLO, J. E; MAHAJAN, V. B; TSANG, S. H. Gene therapy and genome surgery in the retina. The **Journal of Clinical Investigation**, v. 128, n.6, p. 2177-2188, 2018.

ELBASHIR, S.M.; HARBORTH, J.; LENDECKEL, W.; YALCIN, A.; WEBER, K.; TUSCHL, T. Duplexes of 21-nucleotide RNAs mediate RNA interference in cultured mammalian cells. **Nature**, n. 411, p. 494-498, 2001.

ELIAZ, R. E.; SZOKA, F. C. Liposome-encapsulated doxorubicin targeted to CD44: a strategy to kill CD44-overexpressing tumor cells. **Cancer Research**, n. 61, p. 2592–2601, 2001.

ENGLANDER, M.; CHEN, T. C.; PASCHALIS, E. I.; MILLER, J. W.; KIM, I. K. Intravitreal injections at the Massachusetts Eye and Ear Infirmary: analysis of treatment indications and postinjection endophthalmitis rates. **British Journal of Ophthalmology,** v. 4, n. 97, p. 460-465, 2013.

ESPOSITO, G.; GENINATTI CRICH, S.; AIME, S. Efficient Cellular Labeling by CD44 Receptor-Mediated Uptake of Cationic Liposomes Functionalized with Hyaluronic Acid and Loaded with MRI Contrast Agents. **ChemMedChem**, v. 3, n. 12, p. 1858-1862, 2008.

FIRE, A.; XU, S.; MONTGOMERY, M.K.; KOSTAS, S.A.; DRIVER, S.E.; MELLO, C.C. Potent and specific genetic interference by double-stranded RNA in Caenorhabditis elegans. **Nature**. n. 391, p.806–811, 1998.

FRISHMAN, L.J.; WANG, M. H. Electroretinogram of Human, Monkey and Mouse. *In:* **Adler's Physiology of the Eye**, 11th ed., New York: Saunders Elsevier, 2011. p. 480-501.

GASPERINI, A. A.; PUENTES-MARTINEZ, X. E.; BALBINO, T. A.; DE PAULA RIGOLETTO, T.; DE SÁ CAVALCANTI CORRÊA, G.; CASSAGO, A.; … CAVALCANTI, L. P. Association between Cationic Liposomes and Low Molecular Weight Hyaluronic Acid. **Langmuir**, v. 11, n. 31, p. 3308-3317, 2015.

GOODMAN, L. S.; GILMAN, A. **As bases farmacológicas da terapêutica.** 12. ed. Rio de Janeiro: McGraw-Hill, 2012.

GREGORIADIS, G. Drug entrapment in liposomes. **FEBS Letter**, v. 36, p. 292–296, 1973.

GUZMAN-ARANGUEZ, A.; LOMA, P.; PINTOR, J. Small-interfering RNAs (siRNAs) as a promising tool for ocular therapy. **British Journal of Pharmacology**, v. 4, n. 170, p. 730-747, 2013.

HAMOUDI, M. C.; HENRY, E.; ZERROUK, N.; SCHERMAN, D.; ARNAUD, P.; DEPREZ, E.; ESCRIOU, V. Enhancement of siRNA lipid-based vector stability and siRNA integrity in human serum with addition of anionic polymer adjuvant. **Journal of Drug Delivery Science and Technology**, n. 26, p. 01-09, 2015.

HERRERO-VANRELL, R. Microparticles as Drug Delivery Systems for the Back of the Eye. Drug Product Development for the Back of the Eye. **Advances in the Pharmaceutical Sciences Series,** p. 231-259, 2011.

HILLAIREAU, H.; COUVREUR, P. Nanocarriers' entry into the cell: relevance to drug delivery. **Cellular and Molecular Life Sciences**, v. 66, n. 17, p. 2873-2896, 2009.

HUANG, D.; CHEN, Y. S.; RUPENTHAL, I. D. Overcoming ocular drug delivery barriers through the use of physical forces. **Advanced Drug Delivery Reviews**, v.126, p. 96-112, 2018.

HUANG, X.; CHAU, Y. Intravitreal nanoparticles for retinal delivery. **Drug Discovery Today**. v. 24 n. 08, p. 1510-152, 2019.

HUANG, G.; HUANG, W. Application of hyaluronic acid as carriers in drug delivery. **Drug Delivery**, n. 25, p. 766-772, 2018.

ISSA, P. C.; MACLAREN, R. E. Non-viral retinal gene therapy: a review. **Clinical & Experimental Ophthalmology**, n. 40, p. 39-47, 2011.

JIN, L.; ZENG, X.; LIU, M.; DENG, Y.; HE, N. Current Progress in Gene Delivery Technology Based on Chemical Methods and Nano-carriers. **Theranostics**, v. 3, n. 4, p. 240-255, 2014.

KOO, H.; MOON, H.; HAN, H.; NA, J. H.; HUH, M. S.; PARK, J. H. The movement of self-assembled amphiphilic polymeric nanoparticles in the vitreous and retina after intravitreal injection. **Biomaterials**, v.33, n.12, p. 3485-3493, 2012.

LAJAVARDI, L.; BOCHOT, A.; CAMELO, S.; GOLDENBERG, B.; NAUD, M.C.; BEHAR-COHEN, F.; FATTAL, E.; KOZAK, Y. Downregulation of endotoxin-induced uveitis by intravitreal injection of vasoactive intestinal peptide encapsulated in liposomes, **Investigative Ophthalmology & Visual Science, v.** 48, p. 3230–3238, 2007.

LEINONEN, H.; TANILA, H. Vision in laboratory rodents- Tools to measure it and implications for behavioral research. **Behavioural Brain Research**, p.1-12, 2017.

LIU, H.; LIU, Y.; MA, Z.; WANG, J.; ZHANG, Q. A Lipid Nanoparticle System Improves siRNA Efficacy in RPE Cells and a Laser-Induced Murine CNV Model. **Investigative Opthalmology & Visual Science**, v. 7, n. 52, p. 4789-4794, 2011.

MA, J.; WANG, Y.; WEI, P.; JHANJI, V. Biomechanics and structure of the cornea: implications and association with corneal disorders. **Survey of ophthalmology**, v. 63, p. 851-861, 2018.

MALHOTRA, A. et al. Ocular Anatomy and Cross-Sectional Imaging of the Eye. **Semin Ultrasound CT MRI**, [s.l.], n.32, p. 2-13, 2011.

MANNERMAA, E.; VELLONEN, K-S.; URTTI, A. Drug transport in corneal epithelium and blood-retina barrier: Emerging role of transporters in ocular pharmacokinetics. **Advanced Drug Delivery Reviews,** n. 16, p. 1648-1708, 2006.

MARMOR, M. F. et al. ISCEV Standard for full-field clinical electroretinography.**Documenta Ophthalmologica**, v. 118, n. 1, p.69-77, 2008.

MARTENS, T. F.; REMAUT, K.; DESCHOUT, H.; ENGBERSEN, J. F.; HENNINK, W. E.; VAN STEENBERGEN, M. J.; BRAECKMANS, K. Coating nanocarriers with hyaluronic acid facilitates intravitreal drug delivery for retinal gene therapy. **Journal of Controlled Release**, n. 202, p. 83-92, 2015.

MARTENS, T. F.; PEYNSHAERT, K.; NASCIMENTO, T. L.; FATTAL, E.; KARLSTETTER, M.; LANGMANN, T.; BRAECKMANS, K. Effect of hyaluronic acid-binding to lipoplexes on intravitreal drug delivery for retinal gene therapy. **European Journal of Pharmaceutical Sciences**, n. 103, p. 27-35, 2017.

MARTIN-GIL, A.; DE LARA, M. J.; CROOKE, A.; SANTANO, C.; PERAL, A.; PINTOR, J. Silencing of P2Y2receptors reduces intraocular pressure in New Zealand rabbits. **British Journal of Pharmacology,** v. 4, n. 165, p. 1163-1172, 2012.

MERMOUD A; BAERVELDT, G.; MINCKLER, D. S.; LEE, B.; RAO, N. A. Intraocular Pressure in Lewis Rats. **Investigative Ophthalmology & Visual Science**, v. 35, n. 5, 1994.

MEURE, L. A.; FOSTER, N. R.; DEHGHANI, F. Conventional and Dense Gas Techniques for the Production of Liposomes: A Review. **AAPS PharmSciTech**, v. 9, n. 3, 2008.

METLAPALLY, R.; WILDSOET, C. Scleral Mechanisms Underlying Ocular Growth and Myopia. **Prog Mol Biol Transl Sci.**, v. 134, p.241-248, 2015.

MISHRA, S.; WEBSTER, P.; DAVIS, M. E. PEGylation significantly affects cellular uptake and intracellular trafficking of non-viral gene delivery particles. **European Journal of Cell Biology,** v. 3, n. 83, p. 97-111, 2004.

MITRA, R. N.; ZHENG, M.; HAN, Z. Nanoparticle-motivated gene delivery for ophthalmic application. **Wiley Interdisciplinary Reviews**: Nanomedicine and Nanobiotechnology, n. 8, p. 160-174, 2015.

MOHLIN, C.; SANDHOLMA, K.; EKDAHL, K.N.; NILSSON, B. The link between morphology and complement in ocular disease. **Molecular Immunology**. v. 89, p. 84-99, 2017.

NAYEROSSADAT, N.; MAEDEH,T.; ALI, P. A . Viral and nonviral delivery systems for gene delivery. **Adv Biomed Res.**, v.1, 2012.

OLIVEIRA, A. V.; ROSA DA COSTA, A. M.; SILVA, G. A. Non-viral strategies for ocular gene delivery. **Materials Science and Engineering**, n. 77, p. 1275-1289, 2017.

PASCOLINI, D. MARIOTTI, S.P. Global estimates of visual impairment: 2010. **Br. J. Ophthalmol.**, v. 96, p. 614-618, 2012.

PATTNI, B. S.; CHUPIN, V.V.; TORCHILIN, V.P.   **Chemical reviews**, v. 115, p. 10938−10966, 2015.

PEETERS, L. ; SANDERS, N. N. ; BRAECKMANS, K. ; BOUSSERY, K. ; VAN DE VOORDE, J. ; DE SMEDT, S. C. ; DEMEESTER, J. Vitreous: A barrier to nonviral ocular gene therapy. **Investigative Opthalmology & Visual Science,** v. 10, n. 46, p. 3553-3561, 2005.

PEETERS, L.; SANDERS, N.; DEMEESTER, J.; DE SMEDT, S. Challenges in non-viral ocular gene transfer: **Biochemical Society Transactions**, ,n. 35, p. 47-49, 2007.

PETIT, L.; KHANNA, H.; PUNZO, C. Advances in Gene Therapy for Diseases of the Eye. **Human Gene Therapy**, v. 8, n. 27, p. 563-579, 2016.

PITKÄNEN, L.; RUPONEN, M.; NIEMINEN, J.; URTTI, A. Vitreous is a barrier in nonviral gene transfer by cationic lipids and polymers. **Pharmaceutical Research**, ,n. 20, p. 576-583, 2003.

PRESLAND, A.; MYATT, J. Ocular anatomy and physiology relevant to anaesthesia. **Anaesthesia and intensive care medicine**, v. 11, n. 10, p. 438-443, 2010.

RHINN, H.; LARGEAU, C.; BIGEY, P.; KUEN, R.L.; RICHARD, M.; SCHERMAN, D.; ESCRIOU, V. How to make siRNA lipoplexes efficient? Add a DNA cargo. **Biochimica et Biophysica Acta**, v.1790, p.219-230, 2009.

ROSSMILLER, B. P.; RYALS, R. C.; LEWIN, A. S. Gene Therapy to Rescue Retinal Degeneration Caused by Mutations in Rhodopsin. **Methods in Molecular Biology**, ,n. 1271, p. 391-410, 2015.

SAGRISTÁ, M. L.; MORA, M.; MADARIAGA, M. A. Surface modified liposomes by coating with charged hydrophilic molecules. **Cellular & Molecular Biology Letters**, ,n. 5, p. 19-33, 2000.

SANDERS, N. N.; PEETERS, L.; LENTACKER, I.; DEMEESTER, J.; DE SMEDT, S. C. Wanted and unwanted properties of surface PEGylated nucleic acid nanoparticles in ocular gene transfer. **Journal of Controlled Release**, v. 3, n. 122, p. 226-235, 2007.

SARAIVA, S.M.; CASTRO-LÓPEZ, V.; PAÑEDA, C.; ALONSO, M.J. Synthetic nanocarriers for the delivery of polynucleotides to the eye. **European Journal of Pharmaceutical Sciences**, n. 103, p. 05–18, 2017.

SARETT, S.M.; NELSON, C.E.; DUVALL, C.L . Technologies for controlled, local delivery of siRNA. **Journal of controlled release**, v. 218, p. 94-113, 2015.

SCHLEGEL, A.; BIGEY, P.; DHOTEL, H.; SCHERMAN, D.; ESCRIOU, V. Reduced in vitro and in vivo toxicity of siRNA-lipoplexes with addition of polyglutamate. **Journal of Controlled Release**, v.165, p.1-8, 2013.

SHEN, J.; ZHANG, W.; QI, R., MAO, Z.; SHEN, H. Engineering functional inorganic-organic hybrid systems: Advances in siRNA therapeutics. **Chemical Society Reviews**, v.47, n. 6, p.1969-1995, 2018.

SHI, F.; WASUNGU, L.; NOMDEN, A.; STUART, M. C.; POLUSHKIN, E.; ENGBERTS, J. B.; HOEKS-TRA, D. Interference of poly(ethylene glycol)–lipid analogues with cationic-lipid-mediated delivery of oligonucleotides; role of lipid exchangeability and non-lamellar transitions. **Biochemical Journal**, v. 1, n. 366, p. 333-341, 2002.

SOLINÍS, M. A.; DEL POZO-RODRÍGUEZ, A.; APAOLAZA, P. S.; RODRÍGUEZ-GASCÓN, A. Treatment of ocular disorders by gene therapy. **European Journal of Pharmaceutics and Biopharmaceutics**, n. 95, p. 331-342, 2015.

SONG, L.; AHKONG, Q.; RONG, Q.; WANG, Z.; ANSELL, S.; HOPE, M.; MUI, B. Characterization of the inhibitory effect of PEG-lipid conjugates on the intracellular

delivery of plasmid and antisense DNA mediated by cationic lipid liposomes. **Biochimica et Biophysica Acta (BBA)** - Biomembranes, ,n. 1558, p. 1-13, 2002.

SURACE, C.; ARPICCO, S.; DUFAŸ-WOJCICKI, A.; MARSAUD, V.; BOUCLIER, C.; CLAY, D.; … FATTAL, E. Lipoplexes Targeting the CD44 Hyaluronic Acid Receptor for Efficient Transfection of Breast Cancer Cells. **Molecular Pharmaceutics**, v. 4, n. 6, p. 1062-1073, 2009.

TAETZ, S.; BOCHOT, A.; SURACE, C.; ARPICCO, S.; RENOIR, J.; SCHAEFER, U. F.; … FATTAL, E. Hyaluronic Acid-Modified DOTAP/DOPE Liposomes for the Targeted Delivery of Anti-Telomerase siRNA to CD44-Expressing Lung Cancer Cells. **Oligonucleotides**, v. 2, n. 19, p. 103-116, 2009.

THAKUR, A.; FITZPATRICK, S.; ZAMAN, A.; KUGATHASAN, K.; MUIRHEAD, B.; HORTELANO, G.; SHEARDOWN, H. Strategies for ocular siRNA delivery: Potential and limitations of non-viral nanocarriers. **Journal of Biological Engineering,** ,n. 6 ligne, 2012.

WANG, Y.; RAJALA, A.; RAJALA, R. Lipid nanoparticles for ocular gene delivery. **Journal of Functional Biomaterials**, v. 2, n. 6, p. 379-394, 2015.

WHEELER, J. J.; PALMER, L.; OSSANLOU, M.; MACLACHLAN, I.; GRAHAM, R. W.; ZHANG, Y. P.; … CULLIS, P. R. Stabilized plasmid-lipid particles: construction and characterization. **Gene Therapy**, v. 2, n. 6, p. 271-281, 1999.

WHITEHEAD, K. A.; LANGER, R.; ANDERSON, D. G. Knocking down barriers: advances in siRNA delivery. **Nat Rev Drug Discov**, v. 8, n.2, p. 129-38, 2009.

WOJCICKI, A. D.; HILLAIREAU, H.; NASCIMENTO, T. L.; ARPICCO, S.; TAVERNA, M.; RIBES, S.; … FATTAL, E. Hyaluronic acid-bearing lipoplexes: Physico-chemical characterization and in vitro targeting of the CD44 receptor. **Journal of Controlled Release**, v. 3, n. 162, p. 545-552, 2012.

XIA, Y.; TIAN, J.; CHEN, X. Effect of surface properties on liposomal siRNA delivery. **Biomaterials**, n. 79, p. 56-68, 2016.

YUE, L.; WEILAND, J. D.; ROSKA, B.; HUMAYUN, M.S. Retinal stimulation strategies to restore vision: Fundamentals and systems**. Progress In Retinal And Eye Research**, v.53, p.21-47, 2016.

YU-WAI-MAN, C.; TAGALAKIS, A. D.; MANUNTA, M. D.; HART, S. L.; KHAW, P. T. Receptor-targeted liposome-peptide-siRNA nanoparticles represent an efficient delivery

system for MRTF silencing in conjunctival fibrosis. **Scientific Reports**, v. 6, n. 1, p. 01-11, 2016.

ZULLIGER, R.; CONLEY, S. M.; NAASH, M. I. Non-viral therapeutic approaches to ocular diseases: An overview and future directions. **Journal of Controlled Release**, v.1, n. 219, p. 471-487, 2015.

ZYLBERBERG, C.; MATOSEVIC, S. Pharmaceutical liposomal drug delivery: a review of new delivery systems and a look at the regulatory landscape. **Drug Delivery**, v. 23, n. 9, p. 3319-3329, 2016.